# Sinkhole Detection and Characterization with 2-D and 3-D Full Waveform Tomography

3-D Sinkhole Imaging Workshop
Gainesville, FL
10/2017

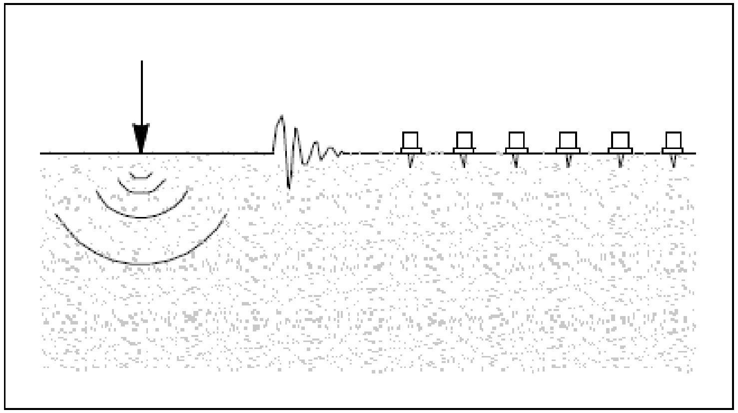


by

Khiem Tran, Ph.D.

Department of Civil and Environmental Engineering
Clarkson University


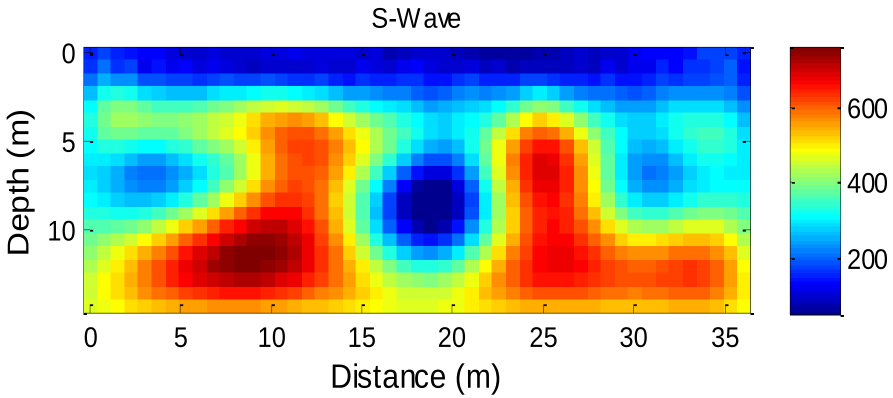

# Outline of presentation

- Need for sinkhole detection
- FWI motivation
- FWI challenges at geotechnical scales
- Overview of FWI methods
- 2-D waveform tomography method
  - Methodology
  - Synthetic data application
  - Florida sinkholes, Ohio abandoned mine voids
- 3-D waveform tomography method
  - 3-D FWI using Adjoint gradient
  - 3-D FWI using Gauss-Newton
  - Synthetic data application
  - First field data application
- Conclusion

# Need of sinkhole detection

## Sinkhole problem

- Structural collapses that lead to significant property damage and even fatalities

## Site investigation

- Typical invasive testing SPT, CPT – tests < .1% of material
- Seismic methods can test over large volume of materials
- Soil/rock property and stratigraphy, and embedded voids/anomalies

Sinkhole collapses

# FWI Motivation

- Most conventional seismic methods analyse travel times of certain wave types
  - inversion of P-wave first arrival travel time
  - inversion of surface wave dispersion
  - migration
  - use only phase, not magnitude
- FWI is <u>wave-equation based</u> and has the potential to
  - use full information content (waveforms), both phase and magnitude
  - consider all measured wave types (P-, S-, Rayleigh waves)
  - **characterize both Vp and Vs at high resolution (meter pixel)**

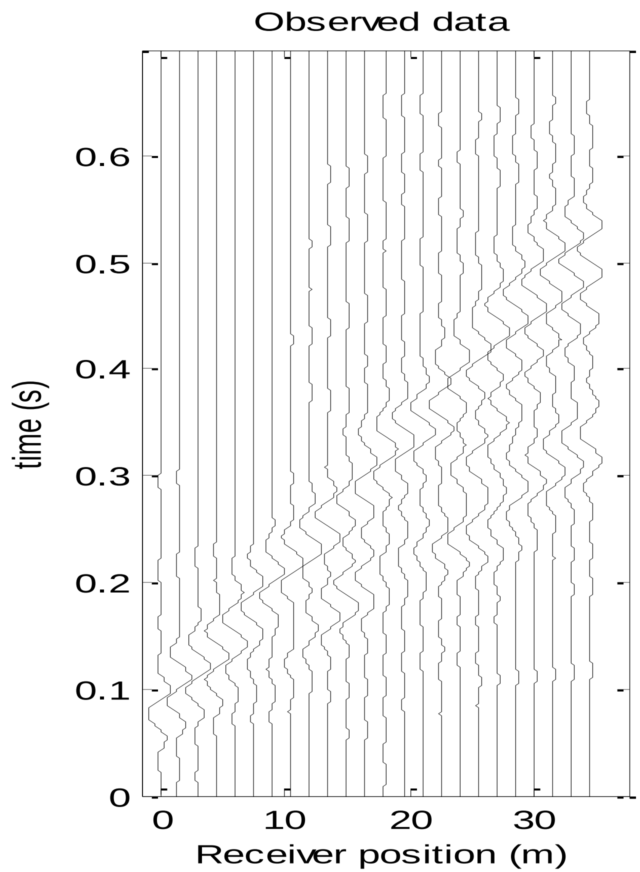


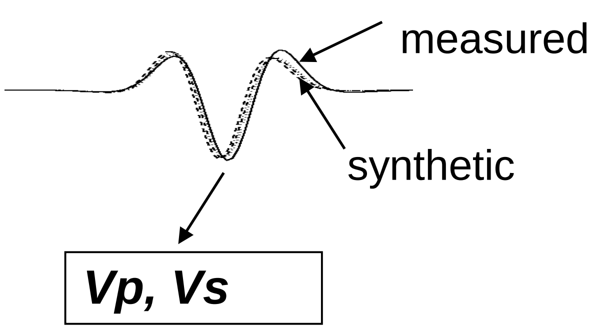

# FWI challenges at geotechnical scales

- inconsistent wave excitation, unknown source signatures (inversion artifacts near source locations)
- strong variability of near surface soil/rock, poor priori information (shallow inversion artifacts, local minimum)
- dominant Rayleigh waves, small body waves with strong attenuation (large model updates at shallow depths, poorly resolved deeper structures)

# Overview of full waveform inversion

**Vs, Vp**
(model **m**)
?

Seismic
testing

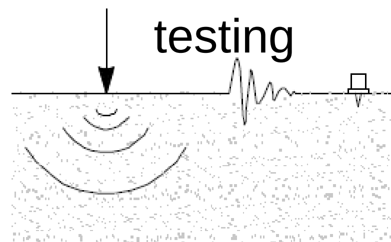

Measured
wave field
**d**

Inverse problem

Inversion method:

- Forward modeling $\mathbf{d} = f(\mathbf{m})$
  - 2-D and 3-D elastic wave equations
    $\longrightarrow \mathbf{d}_{est} = f(\mathbf{m}_{est})$
- Model updating to match $d_{est} \approx \mathbf{d}$
  - Global optimization: simulated annealing, genetic algorithm
  - Deterministic optimization: Gradient, Newton, Gauss-Newton methods

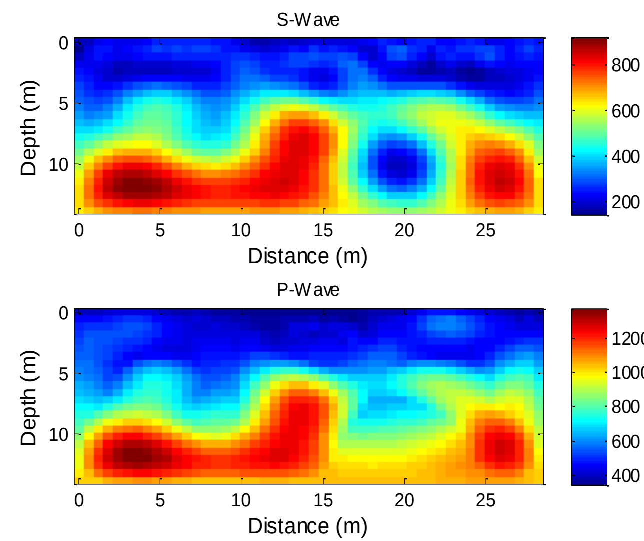

# 2-D FWI

## ➢ Forward modeling

- Eq. governing particle velocity:

$$\begin{cases} \dfrac{\partial v_x}{\partial t} = \dfrac{1}{\rho}\left(\dfrac{\partial \sigma_{xx}}{\partial x} + \dfrac{\partial \sigma_{xz}}{\partial z}\right) \\ \dfrac{\partial v_z}{\partial t} = \dfrac{1}{\rho}\left(\dfrac{\partial \sigma_{xz}}{\partial x} + \dfrac{\partial \sigma_{zz}}{\partial z}\right) \end{cases}$$

- Eq. governing stress tensor:

$$\begin{cases} \dfrac{\partial \sigma_{xx}}{\partial t} = (\lambda + 2\mu)\dfrac{\partial v_x}{\partial x} + \lambda \dfrac{\partial v_z}{\partial z} \\ \dfrac{\partial \sigma_{zz}}{\partial t} = (\lambda + 2\mu)\dfrac{\partial v_z}{\partial z} + \lambda \dfrac{\partial v_x}{\partial x} \\ \dfrac{\partial \sigma_{xz}}{\partial t} = \mu\left(\dfrac{\partial v_x}{\partial z} + \dfrac{\partial v_z}{\partial x}\right) \end{cases}$$

- Perfectly Matched Layer (PML) at bottom and 2 vertical boundaries

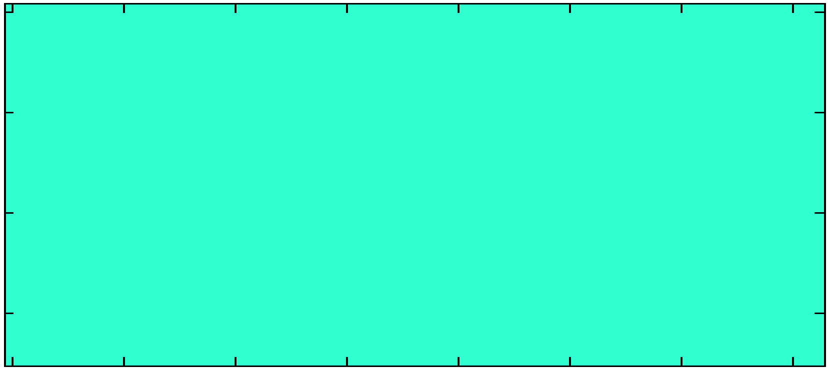

PML

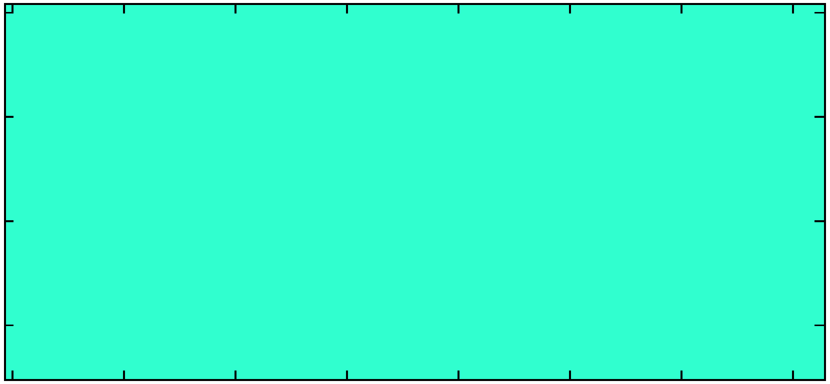

No PML

Tran K.T. and Hiltunen D.R. (2012), “Two-Dimensional Inversion of Full Waveform Using Simulated Annealing”, *Journal of Geotechnical and Geoenvironmental Engineering.*

# 2-D FWI

- Model updating by Gauss-Newton

  - Residual wave field: $$\Delta\mathbf{d}_{i,j} = \mathbf{F}_{i,j}(\mathbf{m}) * \mathbf{d}_{i,k} - \mathbf{d}_{i,j} * \mathbf{F}_{i,k}(\mathbf{m})$$
  - Misfit function: $$\mathrm{E}(\mathbf{m}) = \frac{1}{2}\Delta\mathbf{d}^{t}\,\Delta\mathbf{d}$$

$\mathbf{d}_{i,j}$ and $\mathbf{F}_{i,j}$ ($\mathbf{m}$): measured and estimated data
$\mathbf{d}_{i,k}$ and $\mathbf{F}_{i,k}$ ($\mathbf{m}$): reference traces from measured and estimated data

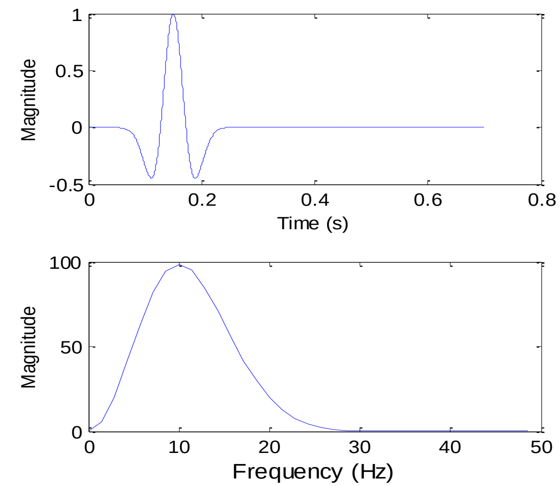


- Source-independence inversion

Tran K.T., McVay M., Horhota D., and Faraone M. (2013), “Sinkhole Detection Using 2D Full Seismic Waveform Tomography”, *Geophysics.*

# 2-D FWI

- Model updating

Filter, focus, balance gradient vector

- Model updating: $$\mathbf{m}^{n+1} = \mathbf{m}^{n} - \alpha^{n} \underbrace{[\mathbf{J}^{t}\mathbf{J} + \lambda_1 \mathbf{P}^{t}\mathbf{P} + \lambda_2 \mathbf{I}^{t}\mathbf{I}]^{-1}}_{\text{Filter, focus, balance gradient vector}} \mathbf{J}^{t} \Delta\mathbf{d},$$

- Jacobian matrix: $$\mathbf{J}_{i,j} = \frac{\partial \mathbf{F}_{i,j}(\mathbf{m})}{\partial m_p} * \mathbf{d}_{i,k} - \mathbf{d}_{i,j} * \frac{\partial \mathbf{F}_{i,k}(\mathbf{m})}{\partial m_p},$$

- Step length: $$\alpha^{n} \cong \frac{[\mathbf{J}^{t} g^{n}]^{t} [\mathbf{F}(\mathbf{m}^{n}) - \mathbf{d}]}{[\mathbf{J}^{t} g^{n}]^{t} [\mathbf{J}^{t} g^{n}]},$$

$$g^{n} = [\mathbf{J}^{t}\mathbf{J} + \lambda_1 \mathbf{P}^{t}\mathbf{P} + \lambda_2 \mathbf{I}^{t}\mathbf{I}]^{-1} \mathbf{J}^{t} [\mathbf{F}(\mathbf{m}^{n}) - \mathbf{d}].$$

Tran K.T., McVay M., Horhota D., and Faraone M. (2013), “Sinkhole Detection Using 2D Full Seismic Waveform Tomography”, *Geophysics.*

# Gauss-Newton vs Adjoint Gradient Method

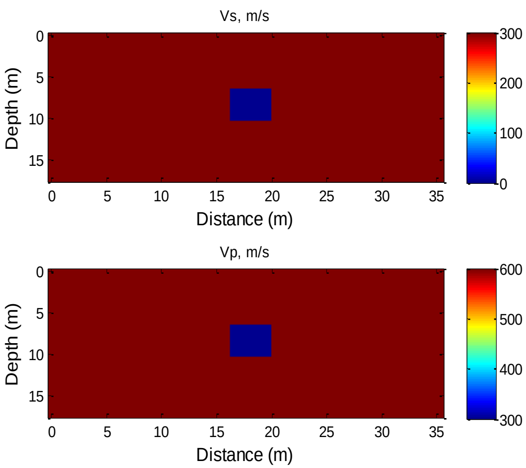


True model

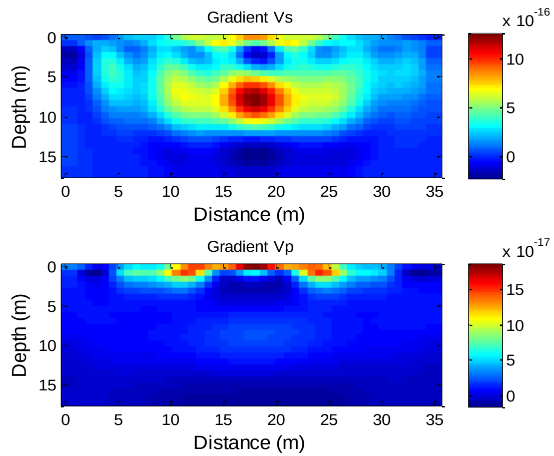


$\mathbf{J}^t \, \Delta\mathbf{d}$

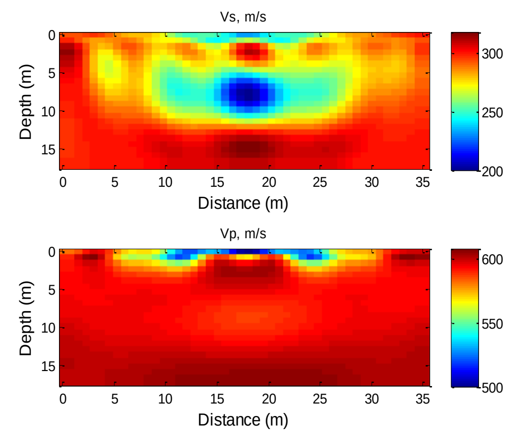


Gradient inverted at first iteration

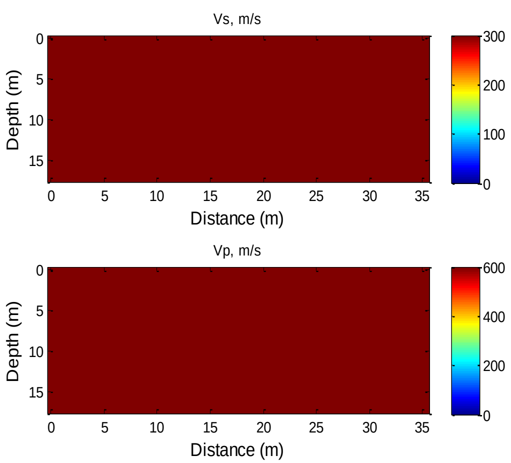


Initial model

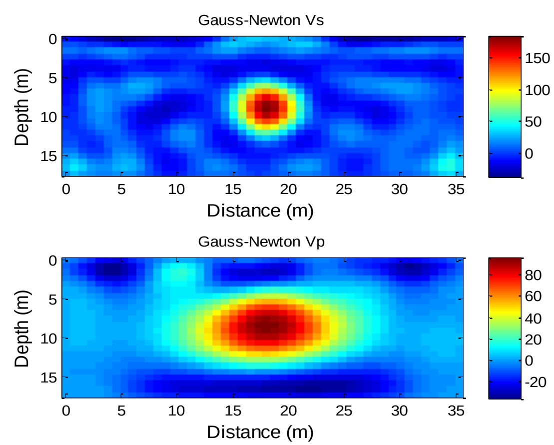


$$[\mathbf{J}^t\mathbf{J} + \lambda_1 \mathbf{P}^t\mathbf{P} + \lambda_2 \mathbf{I}^t\mathbf{I}\,]^{-1}\mathbf{J}^t \, \Delta\mathbf{d}$$

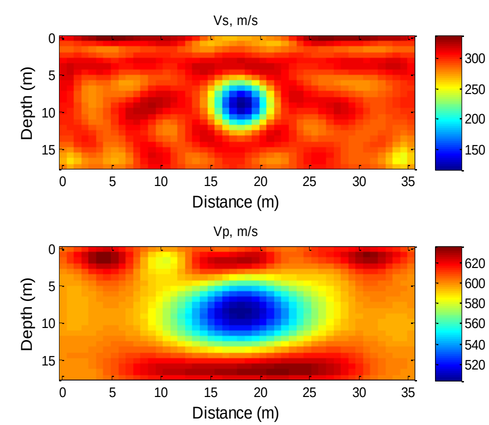


GN inverted at first iteration

# Data Acquisition

- on top of void
- sources & geophones 1 to 3 m spacing
- 10-20 lb. sledgehamm or Propelled energy generator (5-50 Hz signals)
- P-, S-, and Rayleigh waves are all recorded

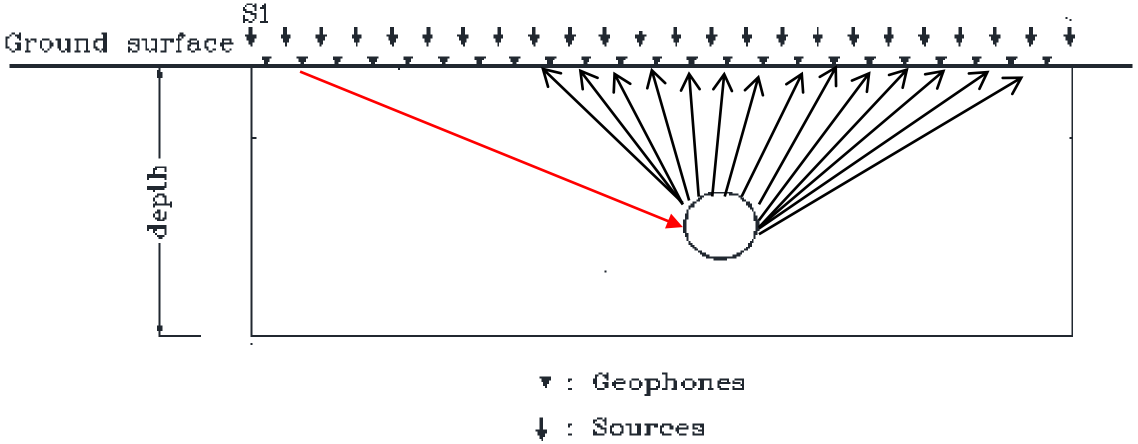


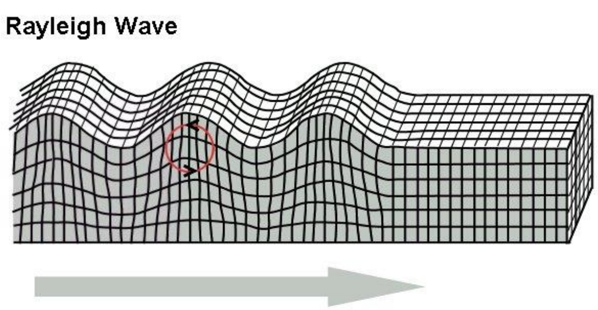


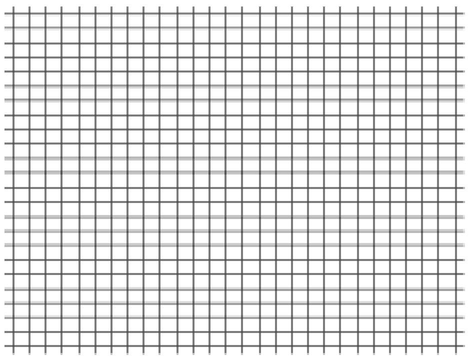

P-wave

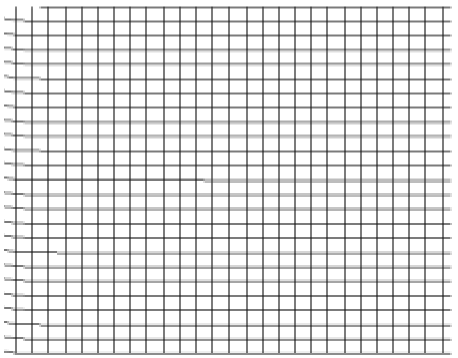

S-wave

# Data Analysis

- Start analysis at lowest frequencies and move up
- Low frequencies (large wavelengths) require less detailed information of initial model
- Adding high frequency data gradually helps to resolve variable near surface structures

Misfit function

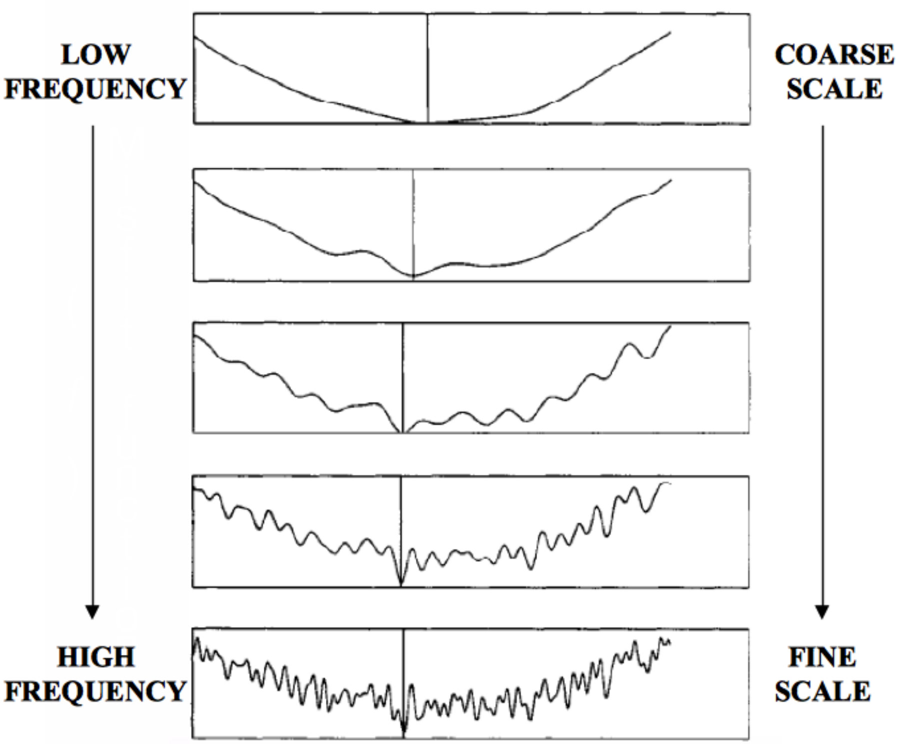


*Bunks et al. (1995)*

# Synthetic Test on Embedded Void

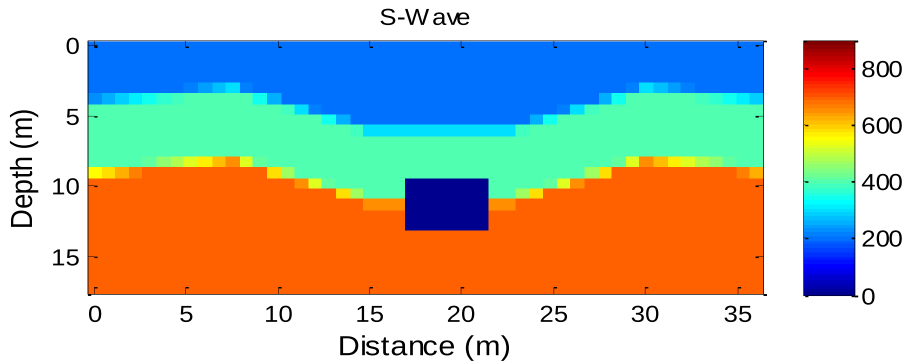


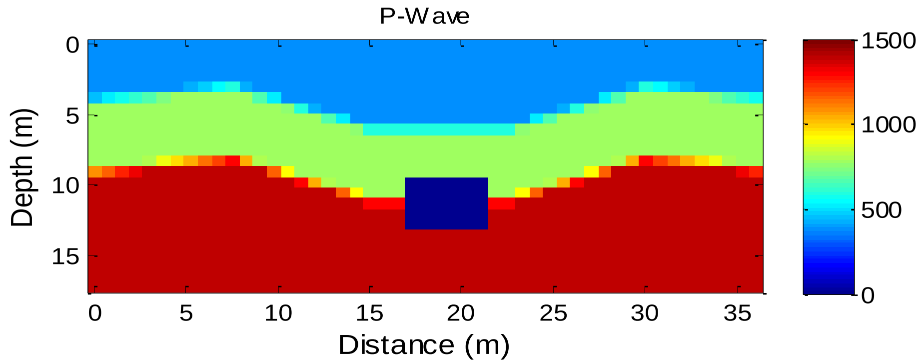


➢ Test configuration

- 24 receivers at 1.5 m spacing
- 25 shots at 1.5 m spacing

- Shot 1

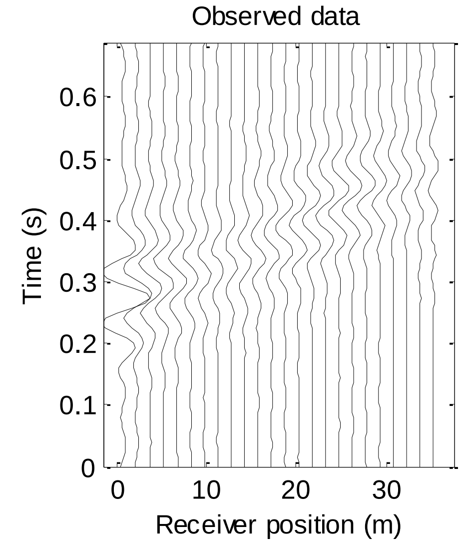


- Shot 13

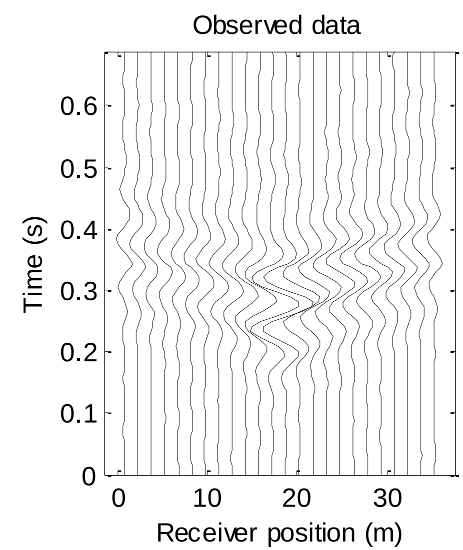

# Synthetic Test on Embedded Void

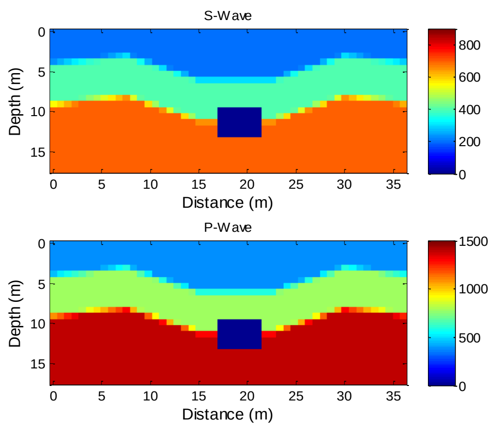


True model

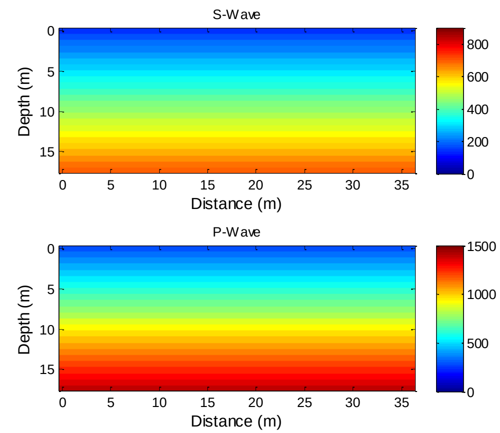


Initial model

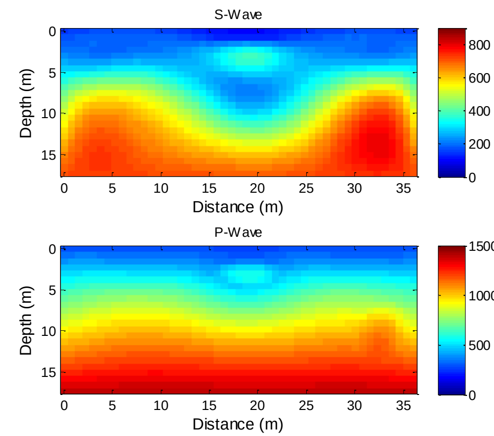


5 Hz

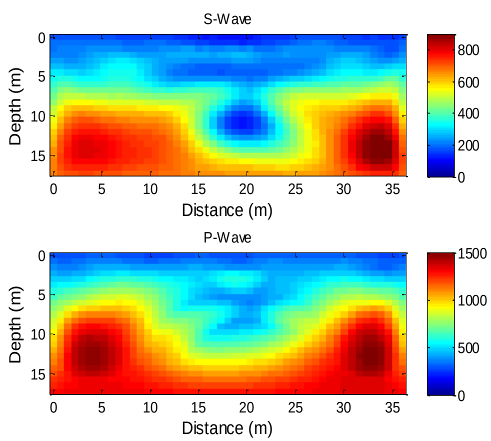


10 Hz

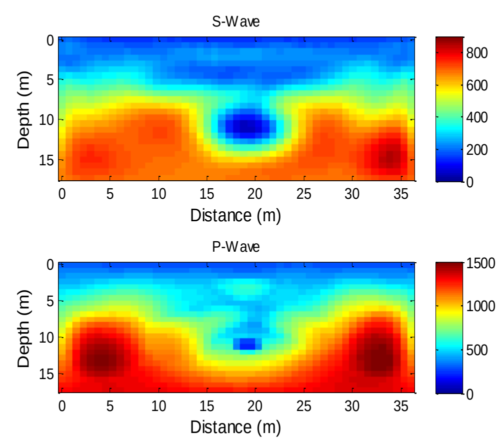


15 Hz

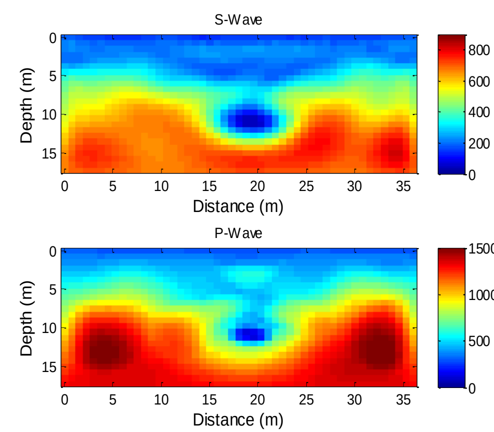


20 Hz

Tran K.T., McVay M., Horhota D., and Faraone M. (2013), "Sinkhole Detection Using 2D Full Seismic Waveform Tomography", *Geophysics.*

# Sinkhole Detection in Florida

- Search for Sinkholes
  - dry retention pond in Newberry, FL
  - fine sand and silt, underlain by highly variable limestone
  - top of limestone varies from 2 m to 10 m in depth
  - no indication of voids on the ground surface
  - 25 lines (A to Y) at 3  m spacing


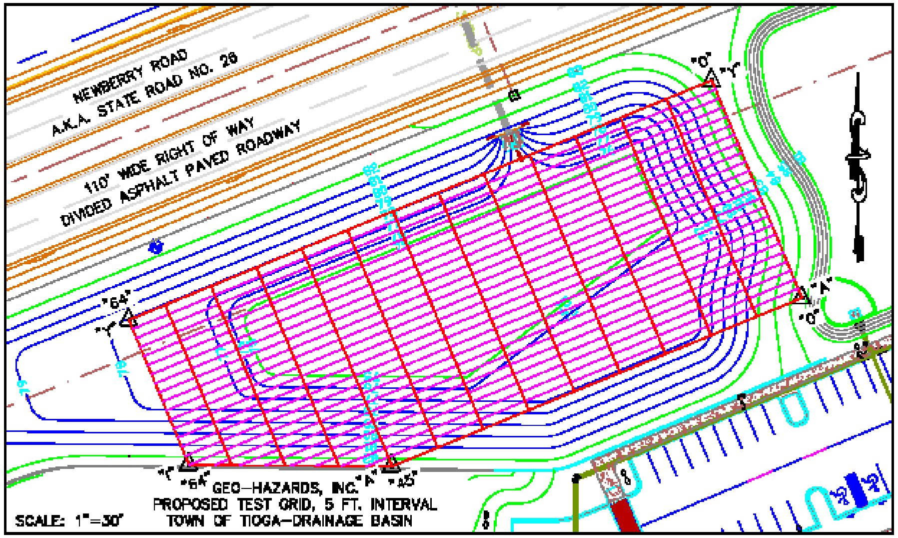

# Newberry, FL

- Search for Sinkholes
  - 10 testing lines at 3 m apart (line K, L, M, N, O, P, Q, R, S, and T)
  - each line 36 m long
  - 24 geophones at 1.5 m spacing
  - 25 shots at 1.5 m spacing
  - 20 lb. sledgehammer for source

# Data Analysis

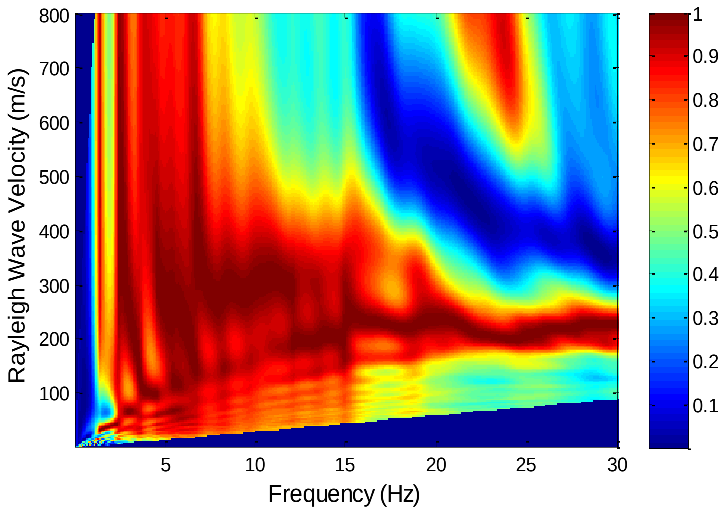


- Power spectrum

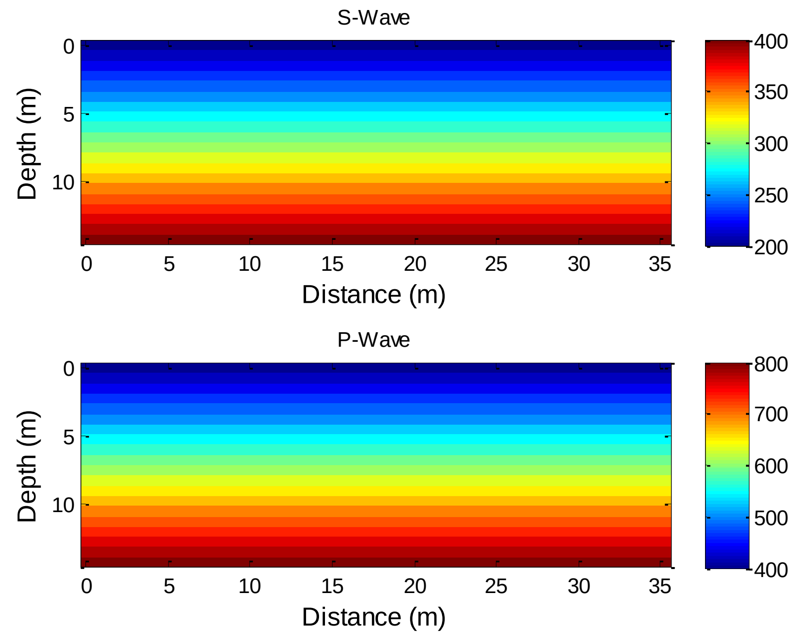


- Initial model

- 4 inversion runs at 6, 10, 15, and 20 Hz central frequencies

# Results of Line P

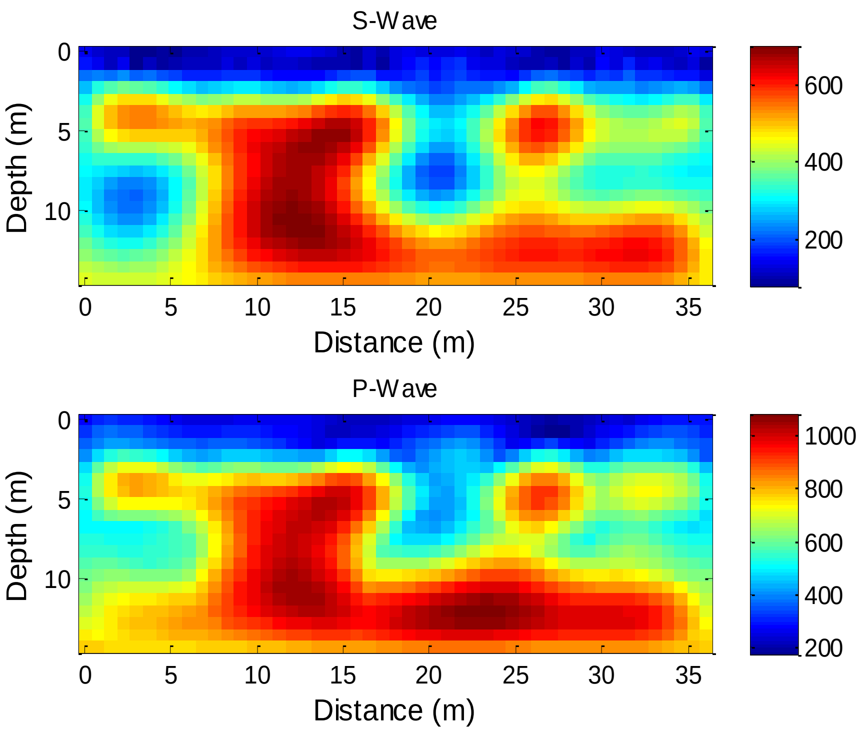


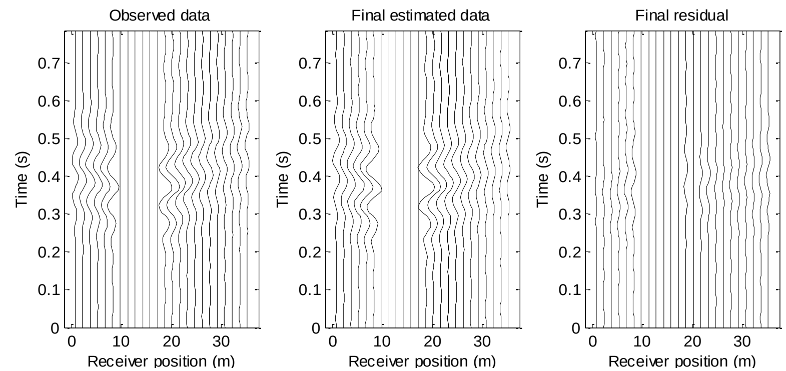


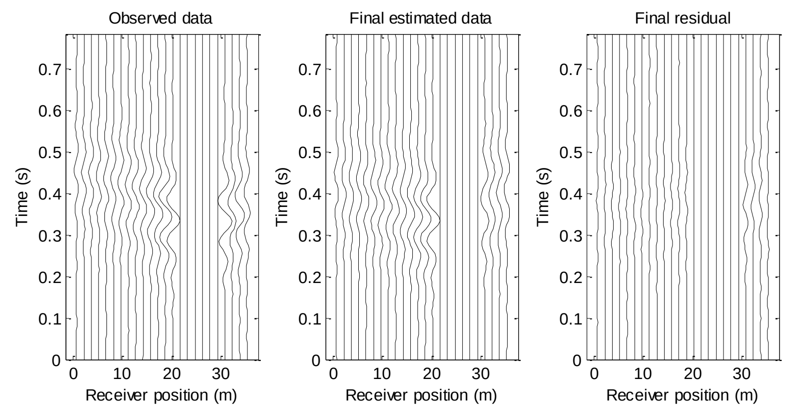

# Results of Line Q

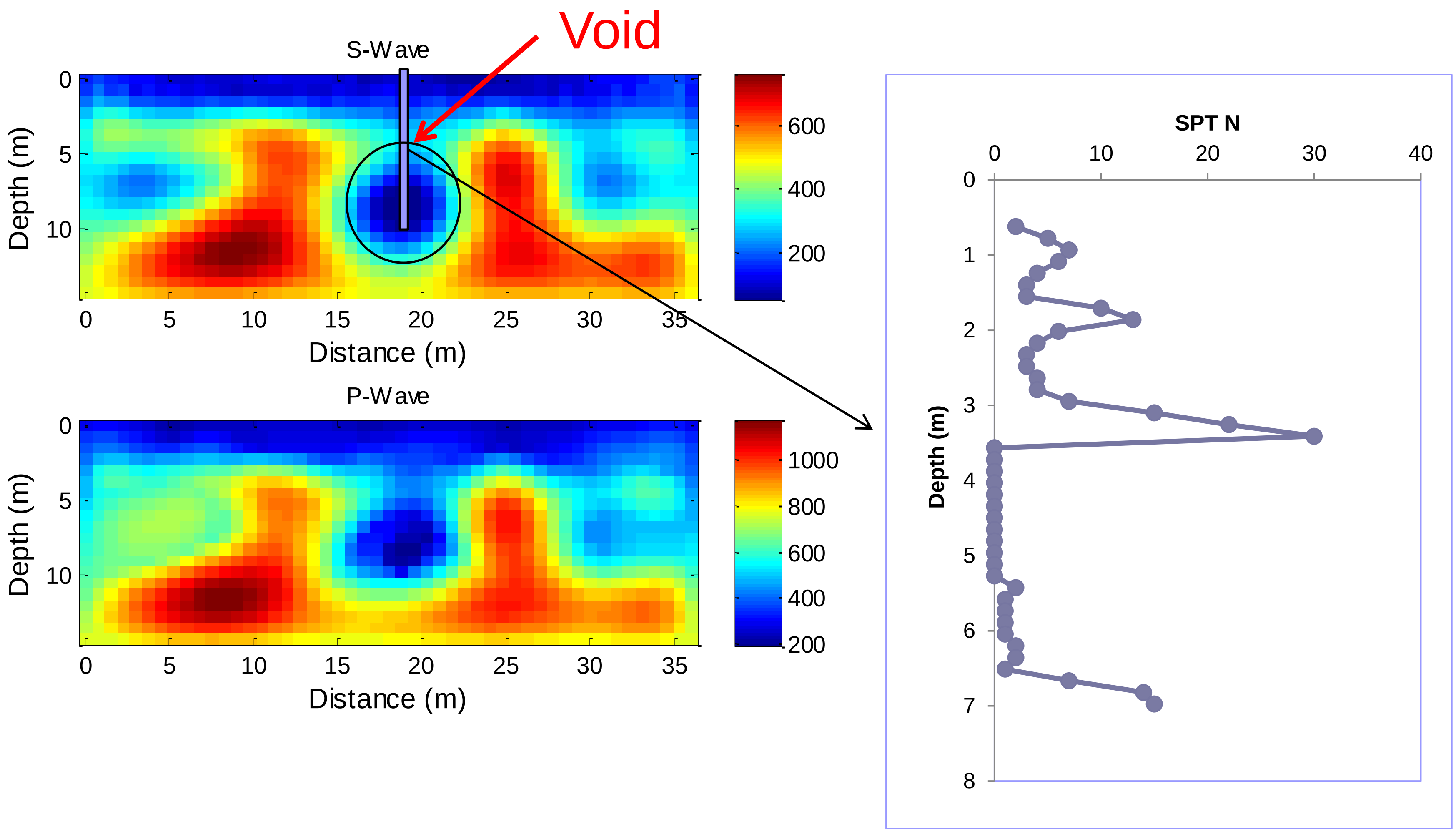


Tran K.T., McVay M., Horhota D., and Faraone M. (2013), “Sinkhole Detection Using 2D Full Seismic Waveform Tomography”, *Geophysics*.

# Abandoned mines in Ohio

➢ Problem

- 8,000 abandoned mines, 1,200 lane miles of Ohio's highway system underlain by mine voids

- Significant risk to the health and safety of the traveling public

- Refraction tomography, GPR, Resistivity, and Micro gravity often fail, because mine voids are deep (40-60 ft in depth)

Subsidence pit on I-70 (Crowell, 2010)

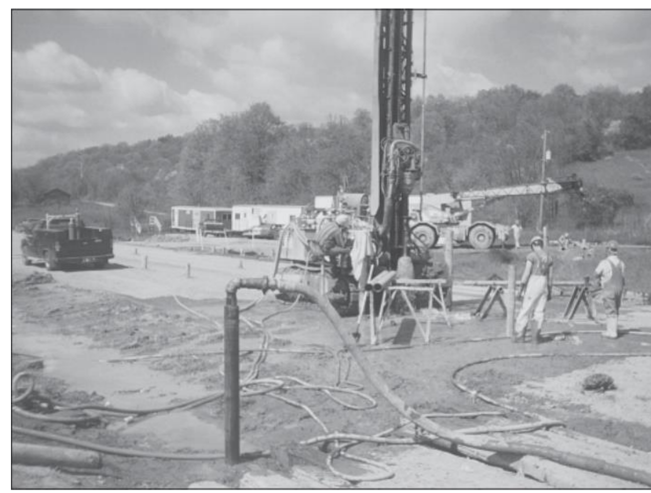

Subsidence stabilization

# US33, Athens, OH

- Search for abandoned mine voids
  - located at the edge of a large abandoned mine complex (no mine map)
  - overburden is interbedded clay shales and sandstones, variable bedrock

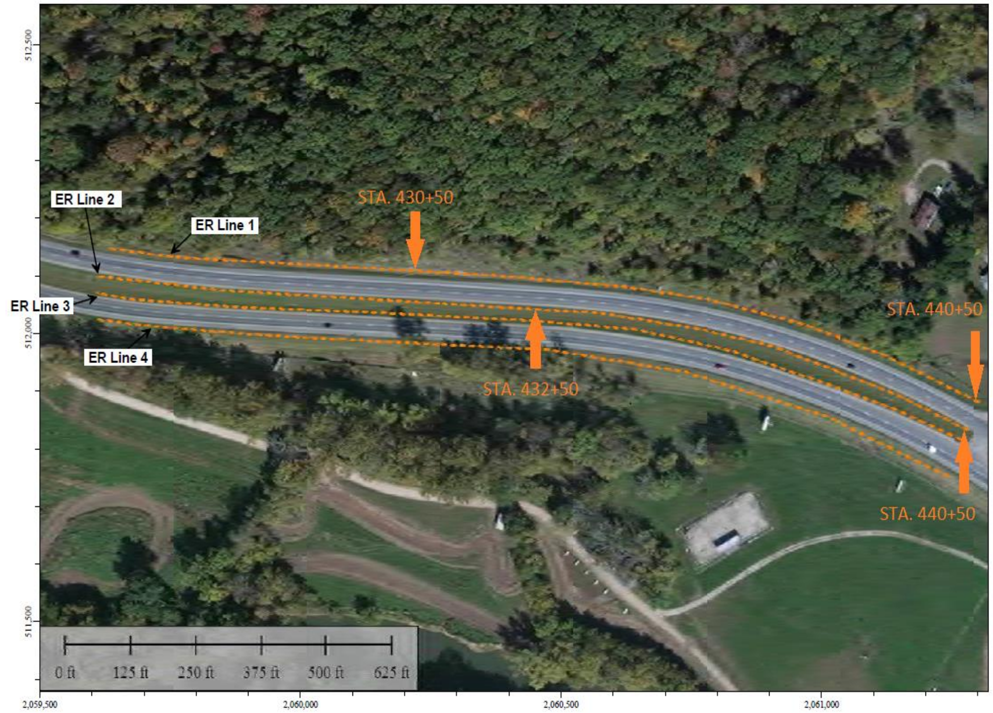

# US33, Athens, OH

- Search for abandoned mine voids

- Land-streamer of 120 ft. length
- 24 geophones at 5 ft. spacing
- Propelled energy generator (PEG 40 kg)
- 2 lines of about 1000 ft. each

**Land-streamer**

Propelled Energy Source

Operator Controlled

# Results: US33, Athens, OH

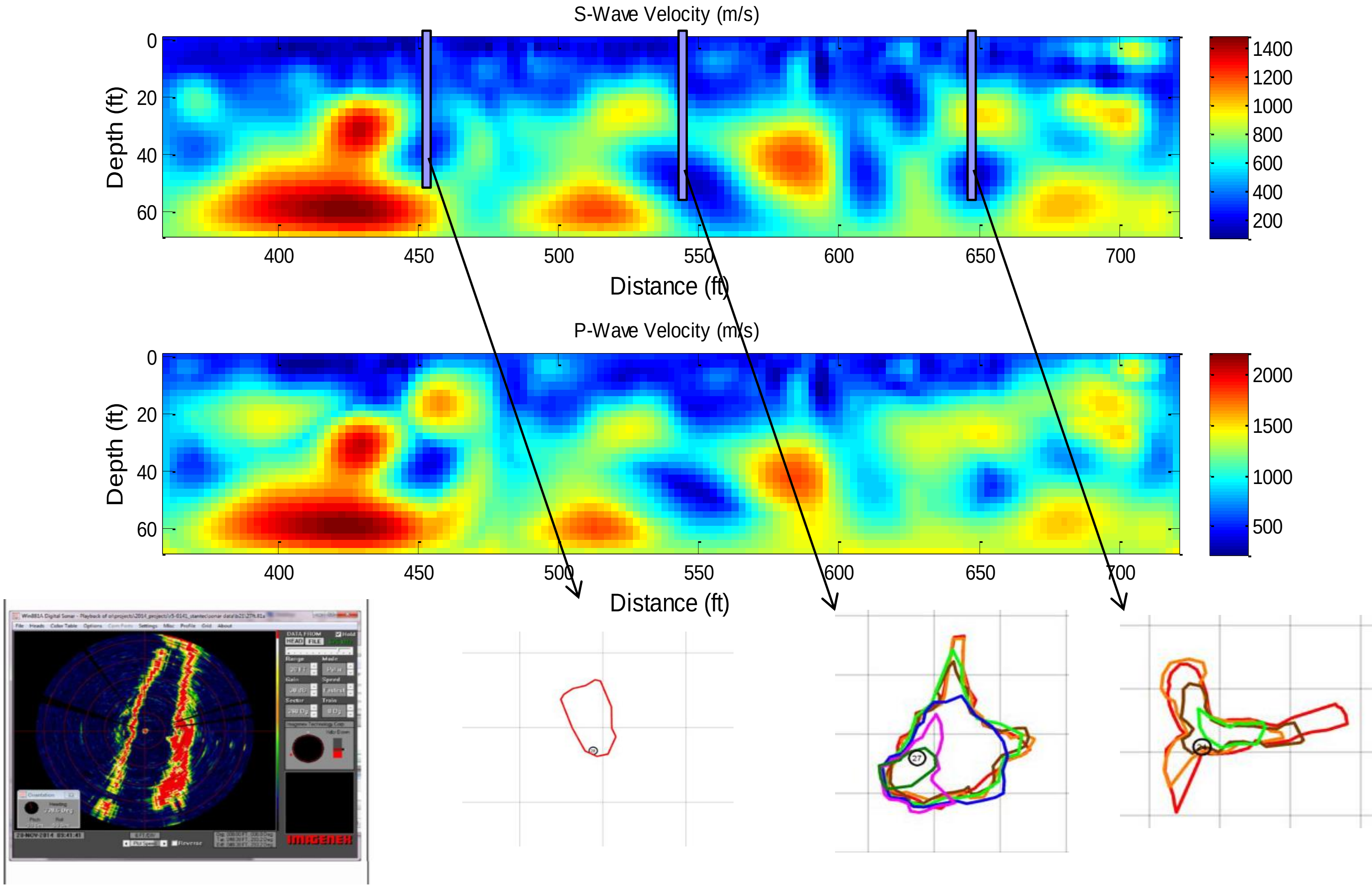


Sullivan B., Tran K.T, and Logston B. (2016), “Characterization of Abandoned Mine Voids Under Roadway Using Land-streamer Seismic Waves”, *Journal of Transportation Research Board*

# Results: US33, Athens, OH

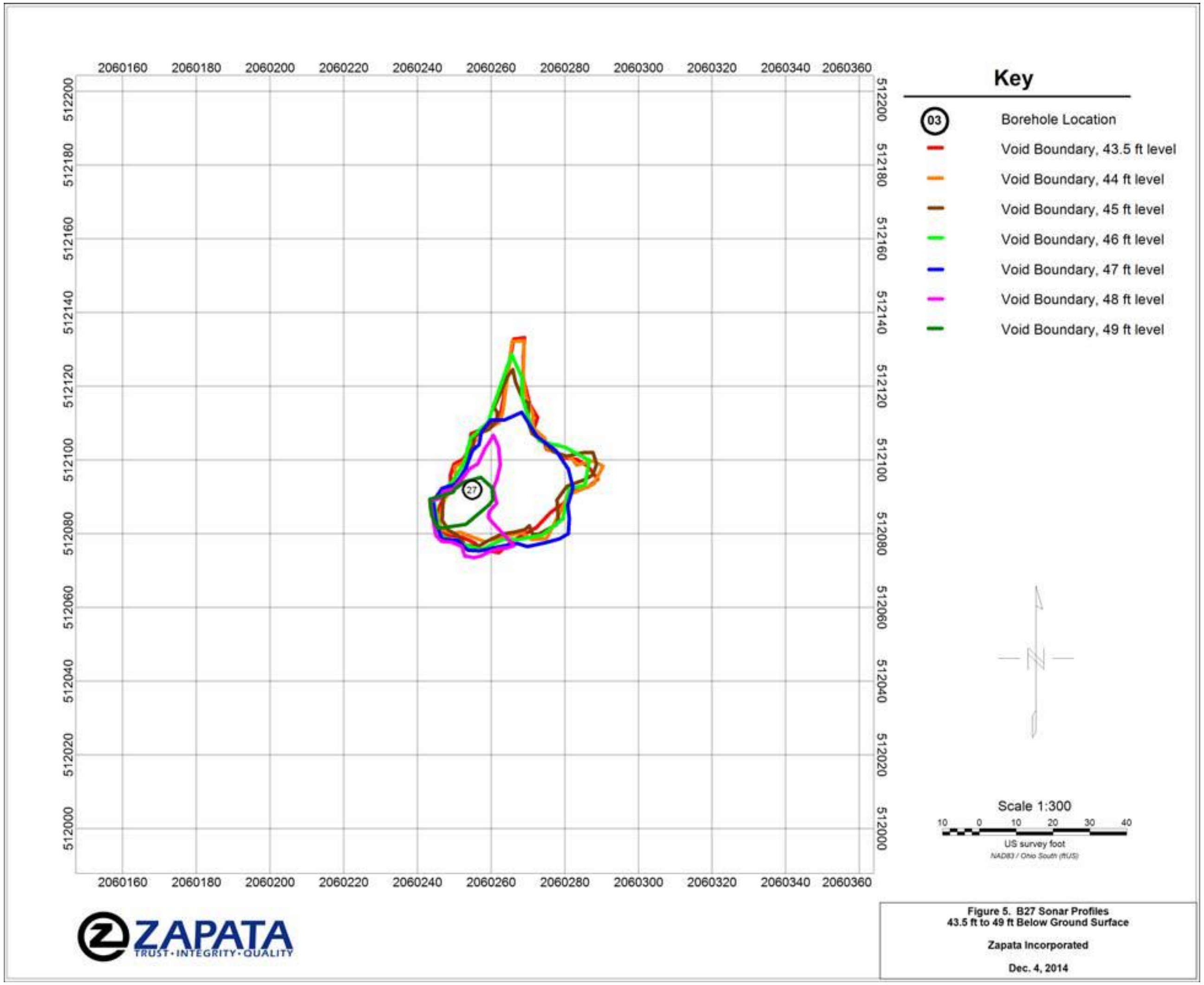

# 3-D FWI

- Forward modeling by 3-D wave equations

$$\rho \frac{\partial v_i}{\partial t} = \frac{\partial \sigma_{ij}}{\partial x_j} + f_i \quad where \;\; i, j = 1,2,3$$

$$\frac{\partial \sigma_{ij}}{\partial t} = \lambda \frac{\partial v_k}{\partial x_k} + 2\mu \frac{\partial v_i}{\partial x_j} \qquad \text{if} \;\; i \equiv j$$

$$\frac{\partial \sigma_{ij}}{\partial t} = \mu \left( \frac{\partial v_i}{\partial x_j} + \frac{\partial v_j}{\partial x_i} \right) \qquad \text{if} \;\; i \neq j$$

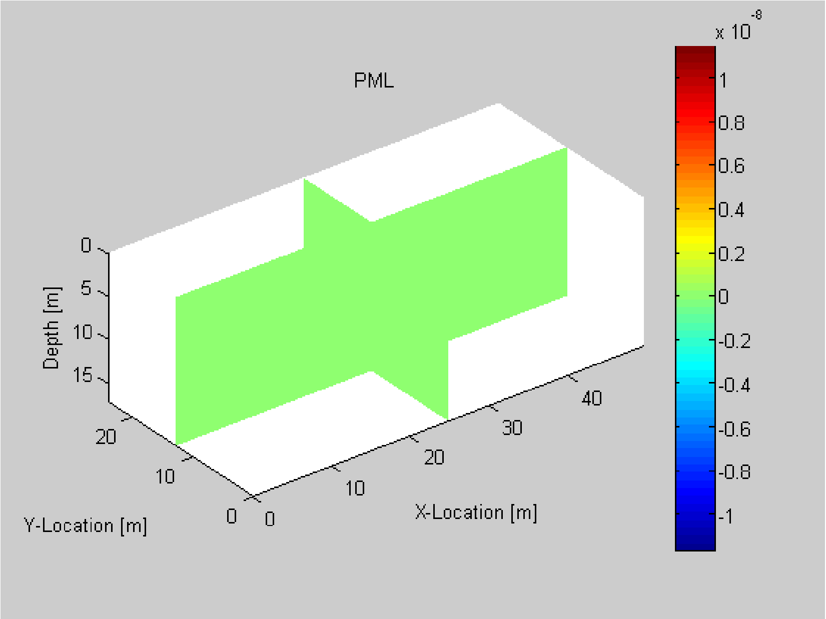


PML is used at bottom and 4 vertical boundaries.


Nguyen D.T. and Tran K.T. (201x), "Site Characterization with 3-D Elastic Full Waveform Tomography", *Geophysics*, under review.

# 3-D FWI

➢ Model updating by Adjoint Gradient

Displacement residual:

$$\Delta u_{i,j}(t) = \int_0^t F_{i,j}(\boldsymbol{m},\tau)d\tau - \int_0^t d_{i,j}(\tau)d\tau$$

Misfit function:

$$E(\boldsymbol{m}) = \frac{1}{2}\Delta\boldsymbol{u}^t\Delta\boldsymbol{u}, \text{ where } \Delta\boldsymbol{u} = \{\Delta u_{i,j}, i = 1,..,NS,\ \ j = 1,..,NR\}$$

Gradients for Lame parameters:

$$\delta\lambda = -\sum_{i=1}^{NS}\int_0^T dt\left[\left(\frac{\partial u_x}{\partial x}+\frac{\partial u_y}{\partial y}\right)\left(\frac{\partial \psi_x}{\partial x}+\frac{\partial \psi_y}{\partial y}\right)+\left(\frac{\partial u_x}{\partial x}+\frac{\partial u_z}{\partial z}\right)\left(\frac{\partial \psi_x}{\partial x}+\frac{\partial \psi_z}{\partial z}\right)+\left(\frac{\partial u_y}{\partial y}+\frac{\partial u_z}{\partial z}\right)\left(\frac{\partial \psi_y}{\partial y}+\frac{\partial \psi_z}{\partial z}\right)\right]$$

$$\delta\mu = -\sum_{i=1}^{NS}\int_0^T dt\left[\begin{array}{c}\left(\frac{\partial u_x}{\partial y}+\frac{\partial u_y}{\partial x}\right)\left(\frac{\partial \psi_x}{\partial y}+\frac{\partial \psi_y}{\partial x}\right)+\left(\frac{\partial u_x}{\partial z}+\frac{\partial u_z}{\partial x}\right)\left(\frac{\partial \psi_x}{\partial z}+\frac{\partial \psi_z}{\partial x}\right)+\left(\frac{\partial u_y}{\partial z}+\frac{\partial u_z}{\partial y}\right)\left(\frac{\partial \psi_y}{\partial z}+\frac{\partial \psi_x}{\partial z}\right)\\ +2\left(\frac{\partial u_x}{\partial x}\frac{\partial \psi_x}{\partial x}+\frac{\partial u_y}{\partial y}\frac{\partial \psi_y}{\partial y}+\frac{\partial u_z}{\partial z}\frac{\partial \psi_z}{\partial z}\right)\end{array}\right]$$

Nguyen D.T. and Tran K.T. (201x), “Site Characterization with 3-D Elastic Full Waveform Tomography”, *Geophysics*, under review.

# 3-D FWI

➢ Model updating by Adjoint Gradient

Gradients for Vs, Vp: $$\delta V_P = 2\rho V_P \delta\lambda$$

$$\delta V_S = -4\rho V_S \delta\lambda + 2\rho V_S \delta\mu$$

Conditioning Gradients:

- tampering to suppress large gradient values near source and receiver locations
- tapering to linearly increase the gradient scales with depth to better resolve deeper structures

Regularization: $$\delta^* V_P = R_{V_P}\,(LV_P) + \ \ \delta V_P$$

$$\delta^* V_S = R_{V_S}\,(LV_S) + \ \ \delta V_S$$

Model update: $${V_P}^{n+1} = {V_P}^{n} - \alpha_P \delta^* V_P$$

$${V_S}^{n+1} = {V_S}^{n} - \alpha_S \delta^* V_S$$

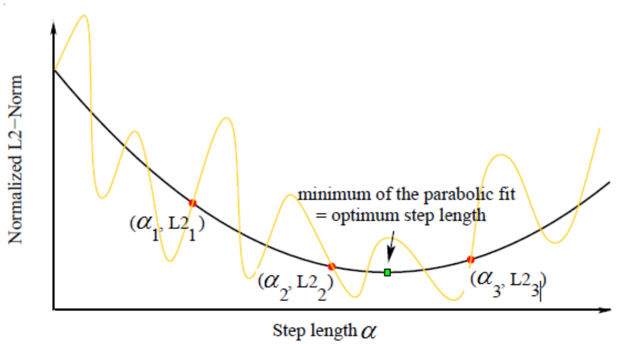

# 3-D FWI

- Model updating by Gauss-Newton

  - Velocity residual: $$\Delta \mathbf{d}_{i,j} = \mathbf{F}_{i,j}(\mathbf{m}) - \mathbf{d}_{i,j}$$
  - Misfit function: $$\mathrm{E}(\mathbf{m}) = \frac{1}{2}\Delta \mathbf{d}^t \, \Delta \mathbf{d}$$
  - Model updating: $$\mathbf{m}^{n+1} = \mathbf{m}^n - \alpha^n [\mathbf{J}^t \mathbf{J} + \lambda_1 \mathbf{P}^t \mathbf{P} + \lambda_2 \mathbf{I}^t \mathbf{I} \,]^{-1} \mathbf{J}^t \, \Delta \mathbf{d},$$
  - Jacobian matrix: $$\mathbf{J}_{i,j} = \frac{\partial \, \mathbf{F}_{i,j}(\mathbf{m})}{\partial \, m_p}$$

  - Gauss-Newton inversion is done in frequency domain to reduce RAM

$$\tilde{u}(\mathbf{x},\omega) = \sum_{l=1}^{nt} \exp(\sqrt{-1}\,\omega l \Delta t) u(\mathbf{x}, l\Delta t)\Delta t$$

# 3-D FWI: Synthetic test

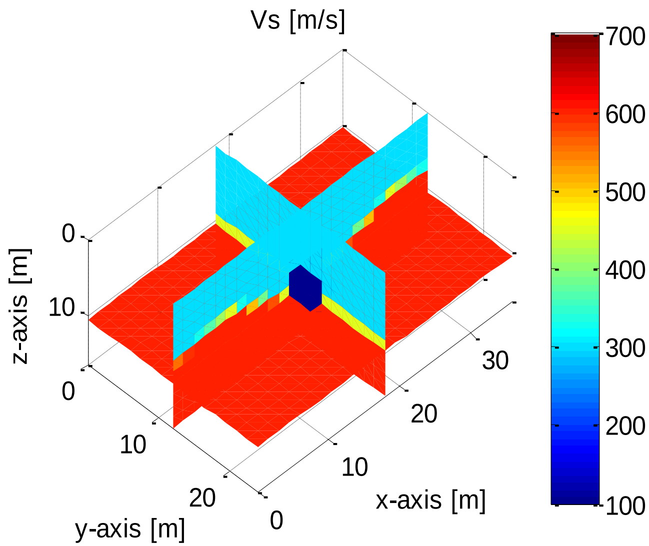


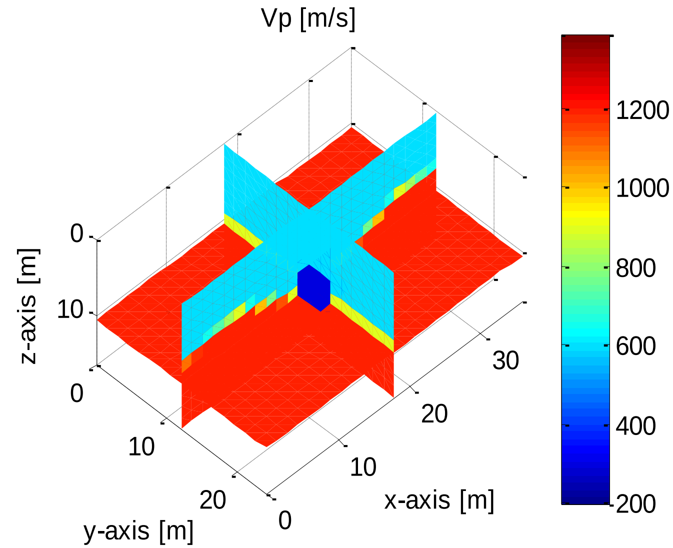


- ➢ 24 x 36 x 18 m model, 4.5x4.5x4.5 m at 9 m depth
- ➢ Test configuration
- 8x12 (96) receivers at 3 m spacing
- 9x13 (117) shots at 3 m spacing

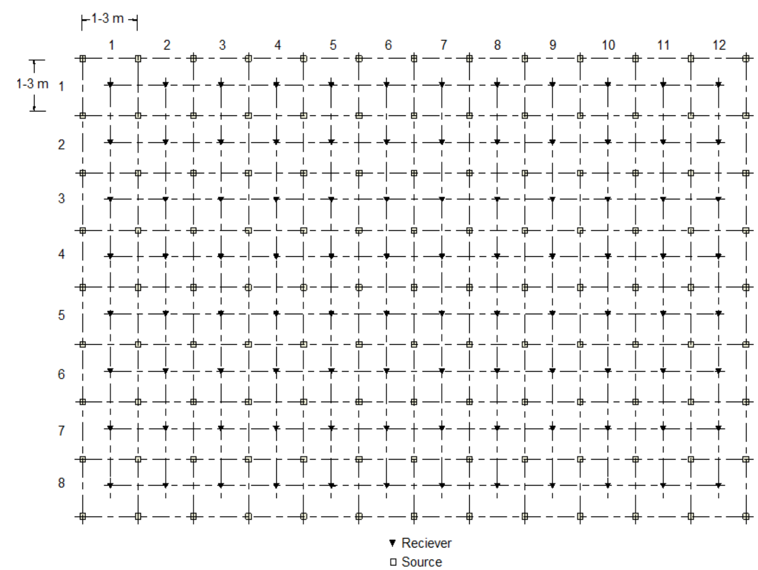

# 3-D FWI: Synthetic test

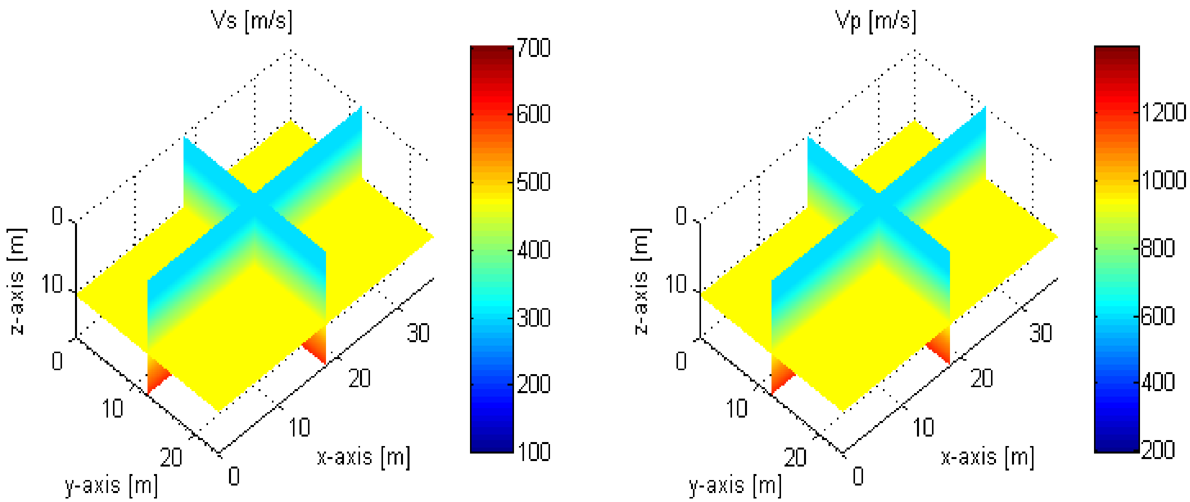


Initial model used for both
Adjoint and GN inversion

- 2 inversion runs at 15 and 25 Hz central frequencies
- about 40 hours for both Adjoint gradient and Gauss-Newton inversions on a desktop computer (32 cores of 3.46 GHz each and 256 GB of memory)

# 3-D FWI: Synthetic test results

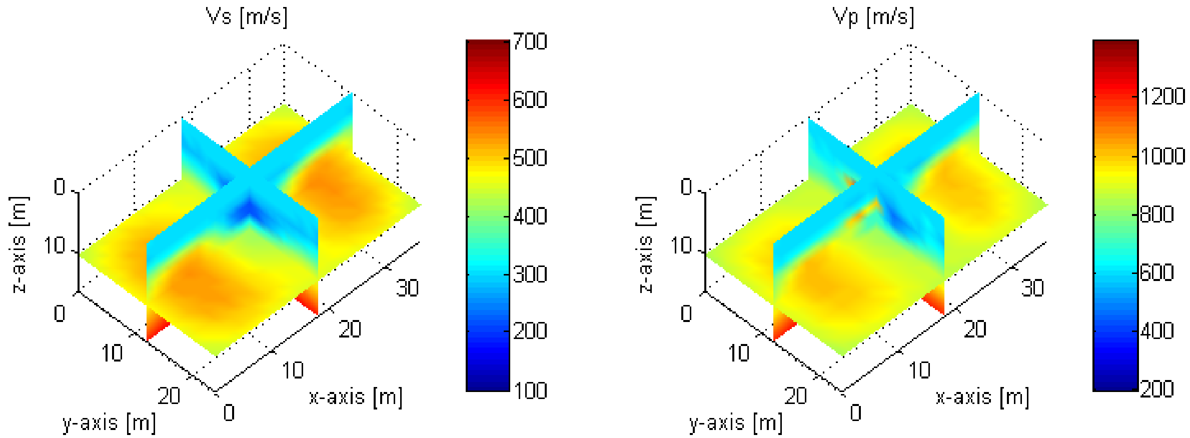


Adjoint gradient

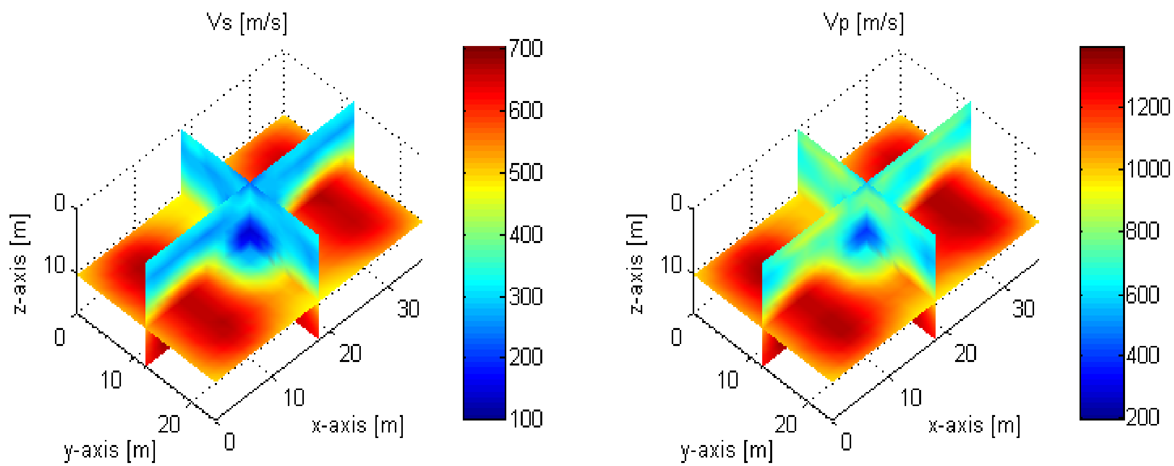


Gauss-Newton

# 3-D FWI: plane comparison at void center

True model

Initial model

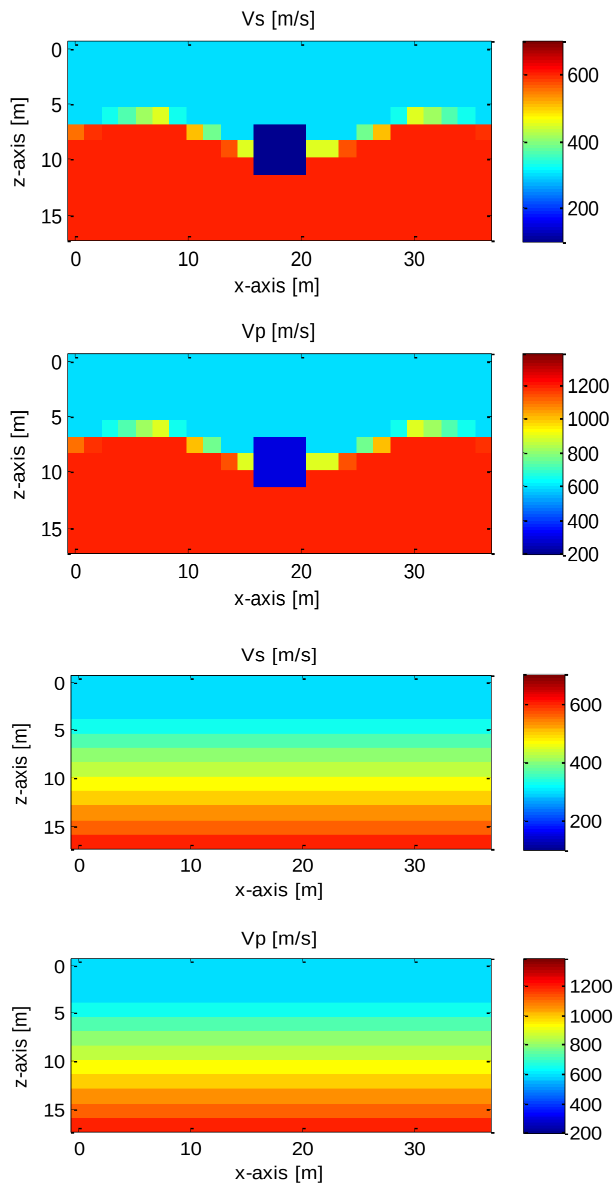


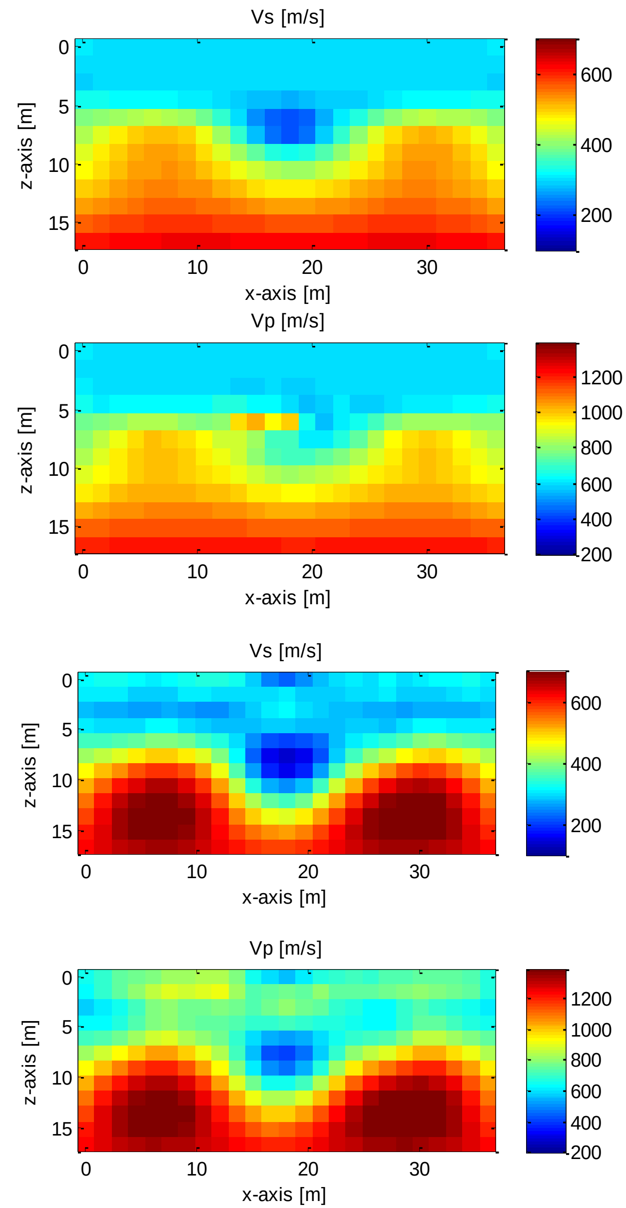


Adjoint gradient

Gauss-Newton

# 3-D FWI: Field data

- dry retention pond in Gainesville
- test area of 36 x 9 m
- 96 receivers located in 24 x 4 grid
- 52 shots located in 13 x 4 grid
- 48 geophones twice
- PEG active source


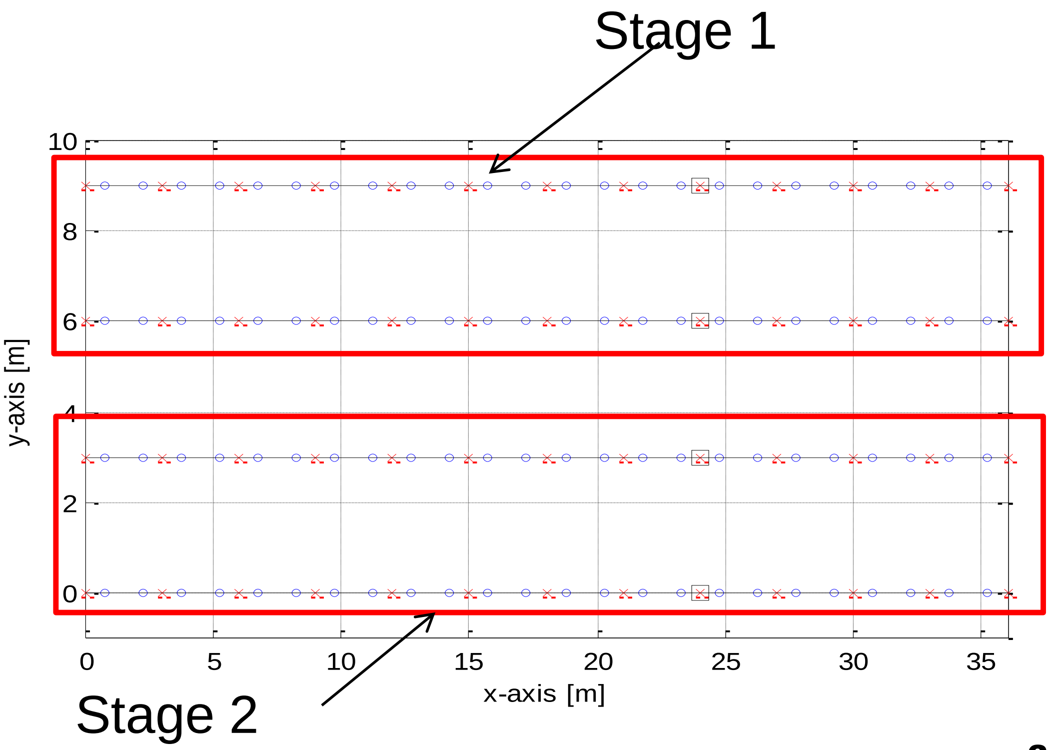

# Sample field data

- measured data combined from the two stages for 96-channel shot gather

- consistent wave magnitudes and propagation pattern

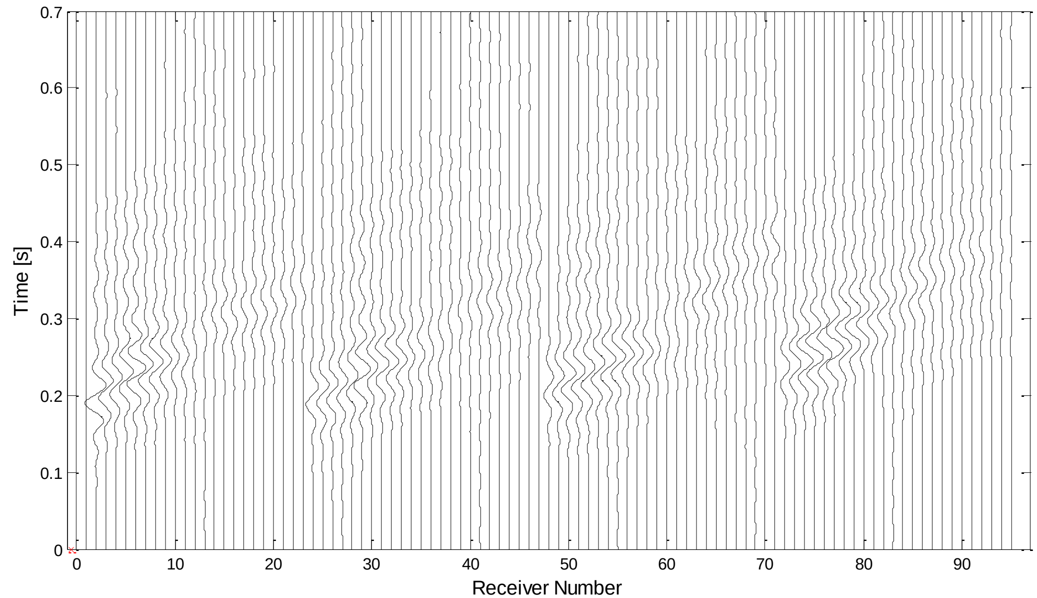


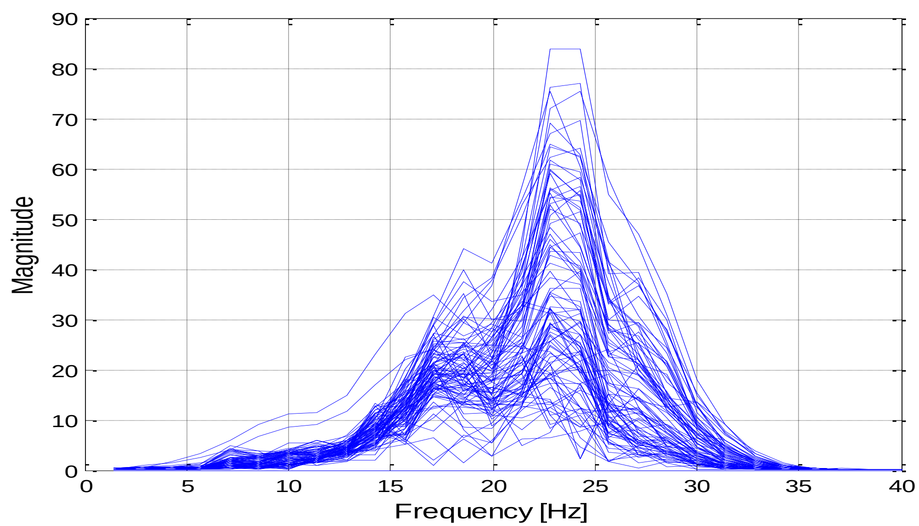

# 3D FWI: Field data analysis

- 2 inversion runs at 12 and 22 Hz central frequencies

- About 30 hours for both Adjoint gradient and Gauss-Newton methods

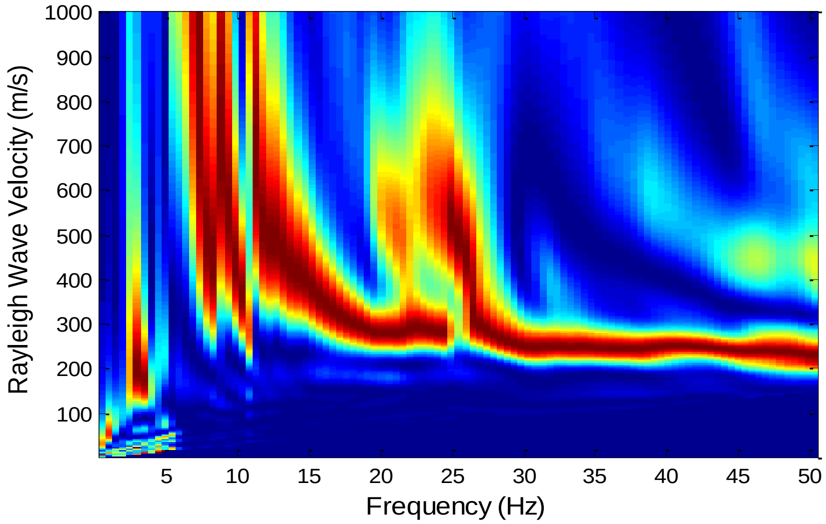


- Power spectrum

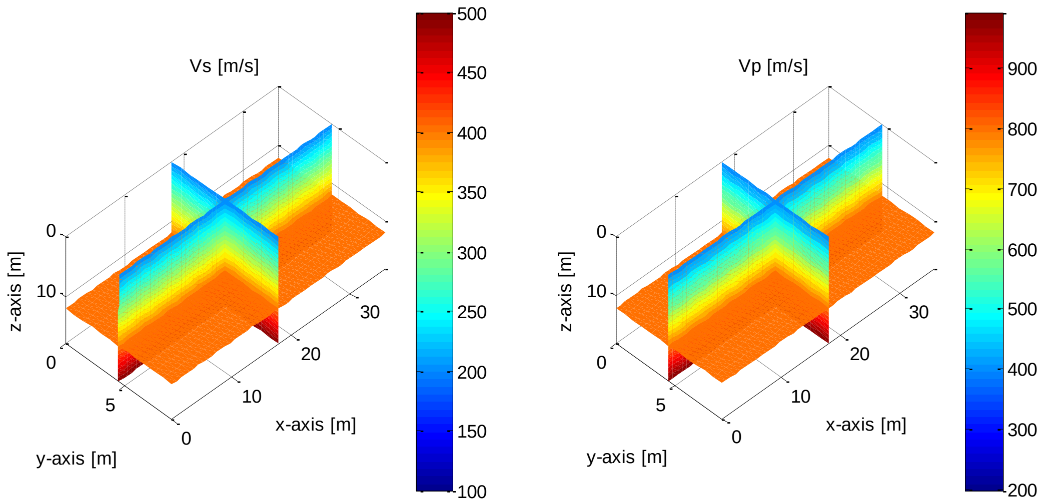


- Initial model

# 3D FWI: Field data analysis

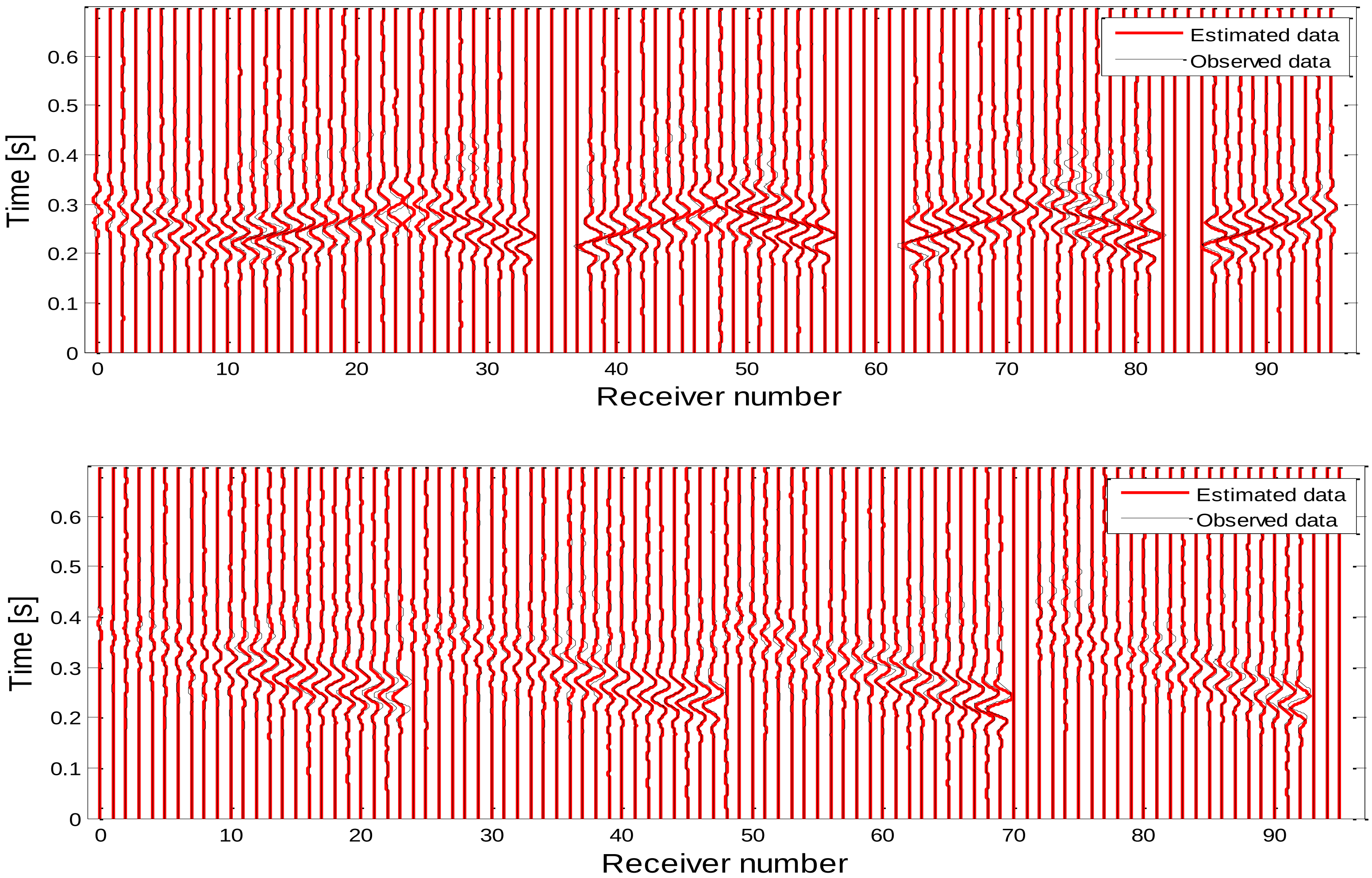


Waveform comparison for 2 sample shots

# 3D FWI: Field data results

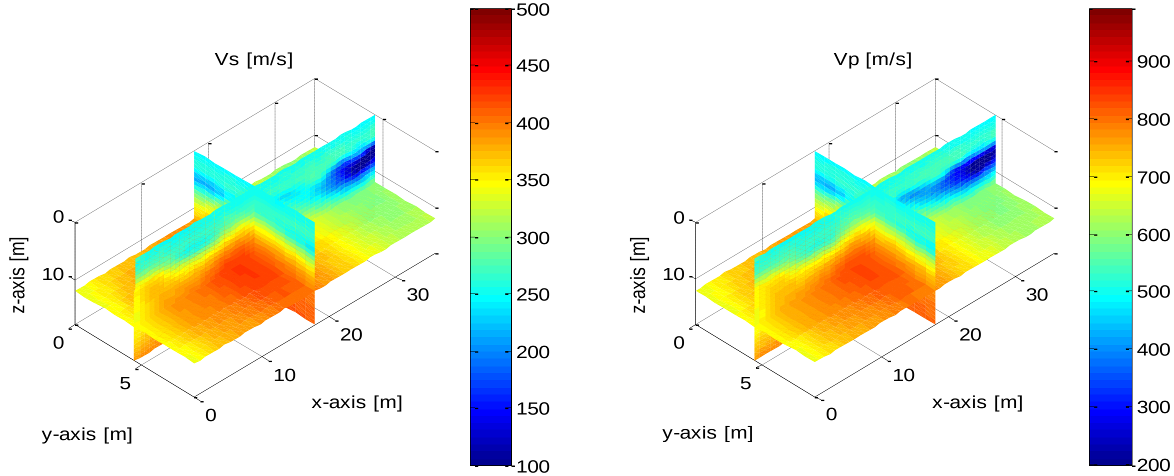


Adjoint gradient

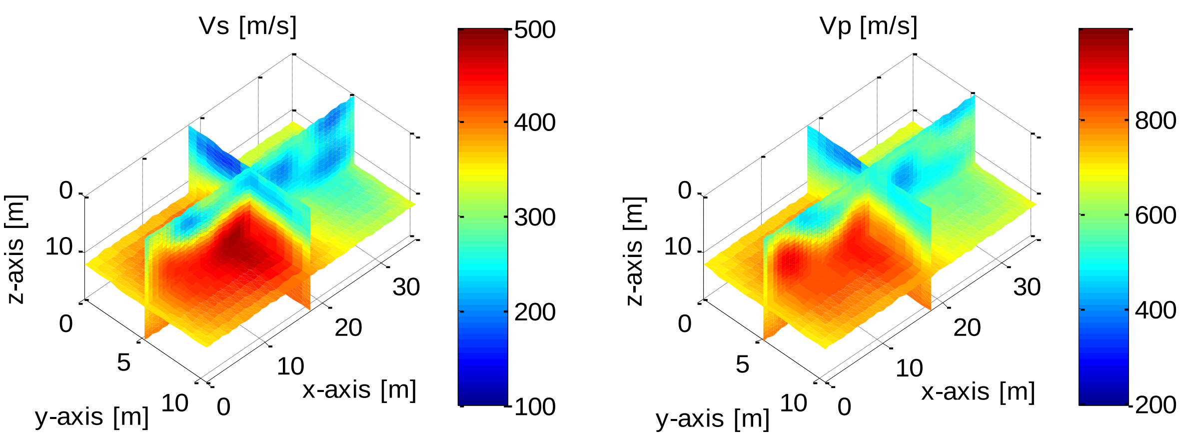


Gauss-Newton

# 3D FWI: Field data results at planes

Gauss-Newton | Adjoint Gradient

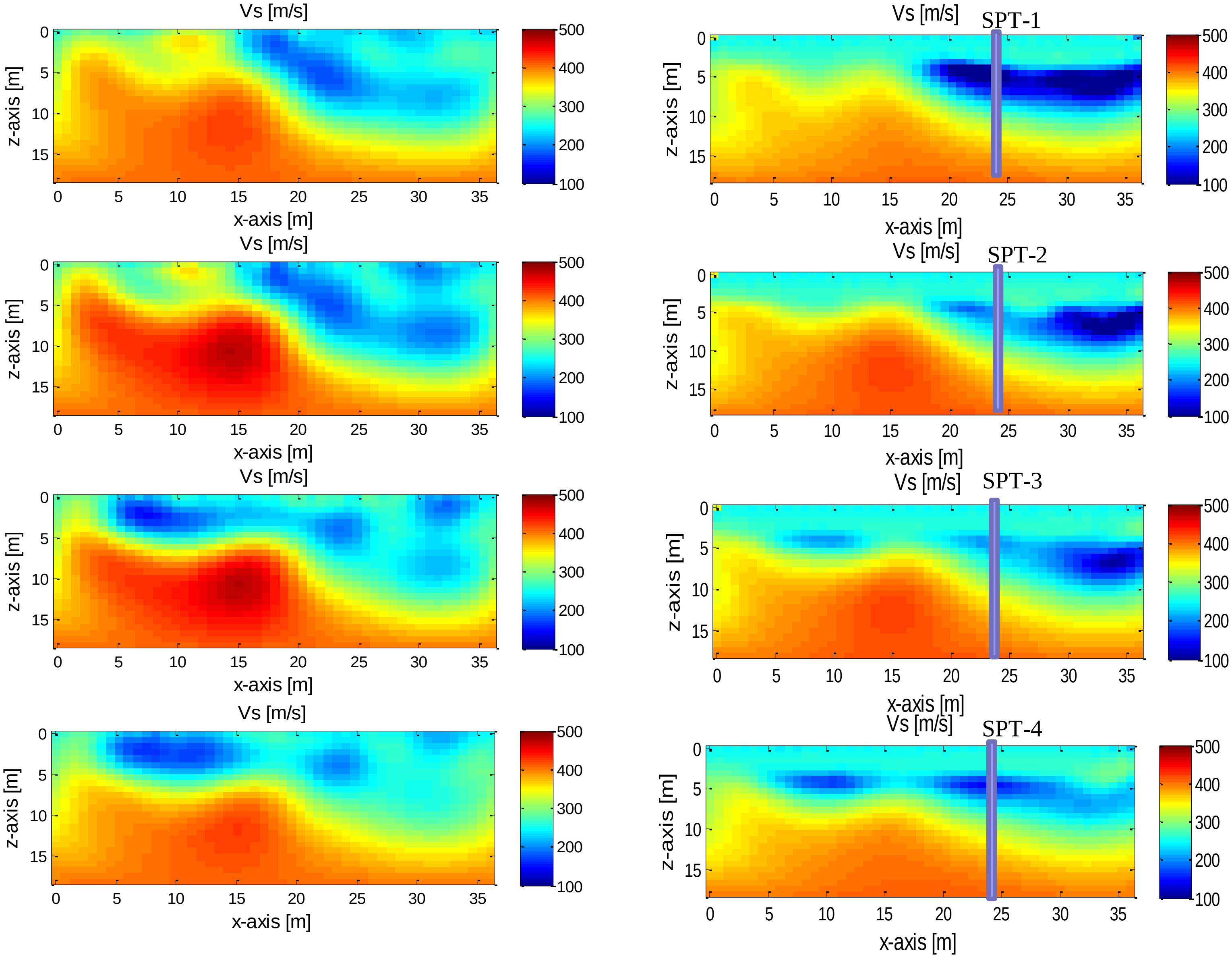


y = 0 m

y = 3 m

y = 6 m

y = 9 m

# 3D FWI vs. SPT results

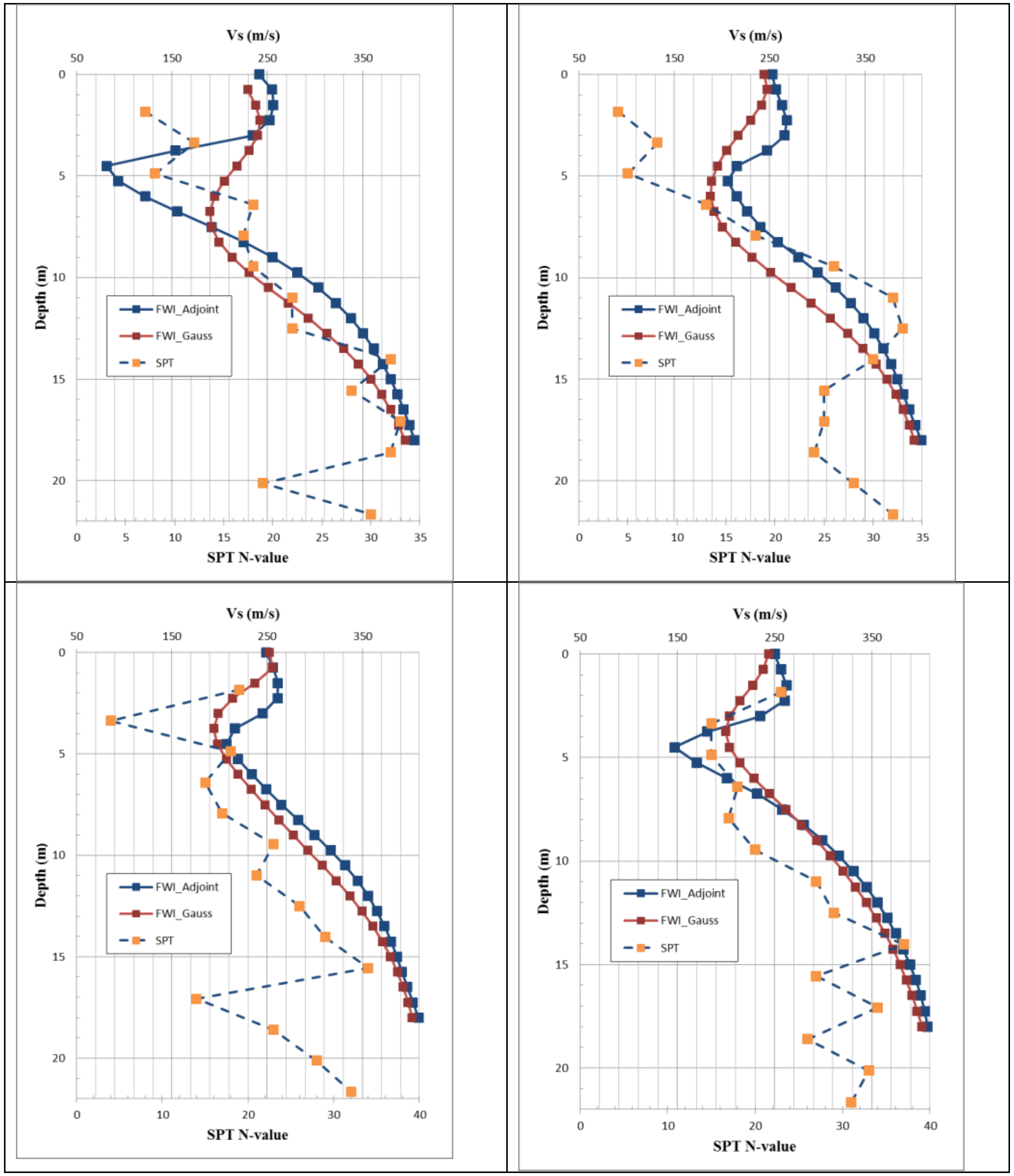

# Conclusion

- Both Vs and Vp can be characterized at high resolution (meter pixel) to 20 m in depth by 2-D and 3-D FWI methods

- Buried void can be identified to a depth of about 3 void diameters with surface measurement

- Gauss-Newton provides better results than Adjoint gradient inversion method, particularly for sinkhole/void imaging

# Future work

- 3-D viscoelastic waveform tomography
- Account for material damping
- Extract more material properties: seismic attenuation Qp, Qs

- 3-D adaptive (non-uniform) mesh waveform tomography
- Begin with uniform mesh to identify low-velocity anomalies
- Use refine mesh only at the anomalies to extract more detailed information

# Acknowledgments

Presented research is funded by FDOT, ODOT, NSF, FHWA

Research team:

- Michael McVay, Dennis Hiltunen, Scott Wasman (UF), David Horhota (FDOT), Khiem Tran (Clarkson)
- Graduate students at Clarkson: Trung Nguyen, Brian Sullivan, Duminidu Siriwardane, Justin Sperry, Majid Mirzanejad, Amila Ambegedara

# References


- Nguyen D.T. and Tran K.T.  (201x), “Site Characterization with 3-D Elastic Full Waveform Tomography”, ***Geophysics***, under review.
- Tran K.T. and Luke B. (2017), “Full Waveform Tomography to Resolve Desert Alluvium”, ***Soil Dynamics and Earthquake Engineering****,* Vol. 9, pp. 1-8.
- Sullivan B., Tran K.T, and Logston B. (2016), “Characterization of Abandoned Mine Voids Under Roadway Using Land-streamer Seismic Waves”, ***Journal of Transportation Research Board***, Vol. 2580, pp. 71-79.
- Tran K.T., McVay M., Horhota D., and Faraone M. (2013), “Sinkhole Detection Using 2D Full Seismic Waveform Tomography”, ***Geophysics***, Vol. 78 (5), pp. R175–R183.
- Tran K.T. and McVay M. (2012), “Site Characterization Using Gauss-Newton Inversion of 2-D Full Seismic Waveform in Time Domain”, ***Soil Dynamics and Earthquake Engineering***, Vol. 43, pp. 16-24.
- Tran K.T. and Hiltunen D.R. (2012), “Two-Dimensional Inversion of Full Waveform Using Simulated Annealing”, ***Journal of Geotechnical and Geoenvironmental Engineering***, Vol. 138(9), pp. 1075-1090.

# *Thank You!*

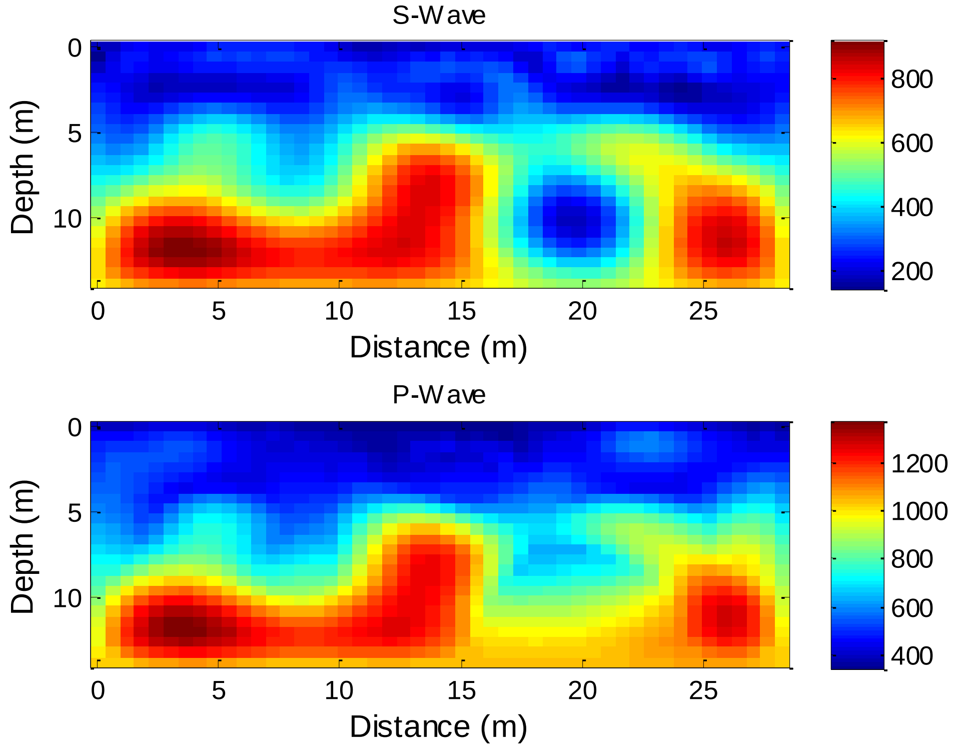
S-Wave
Depth (m)
0
5
10
0
5
10
15
20
25
Distance (m)
800
600
400
200
P-Wave
Depth (m)
0
5
10
0
5
10
15
20
25
Distance (m)
1200
1000
800
600
400